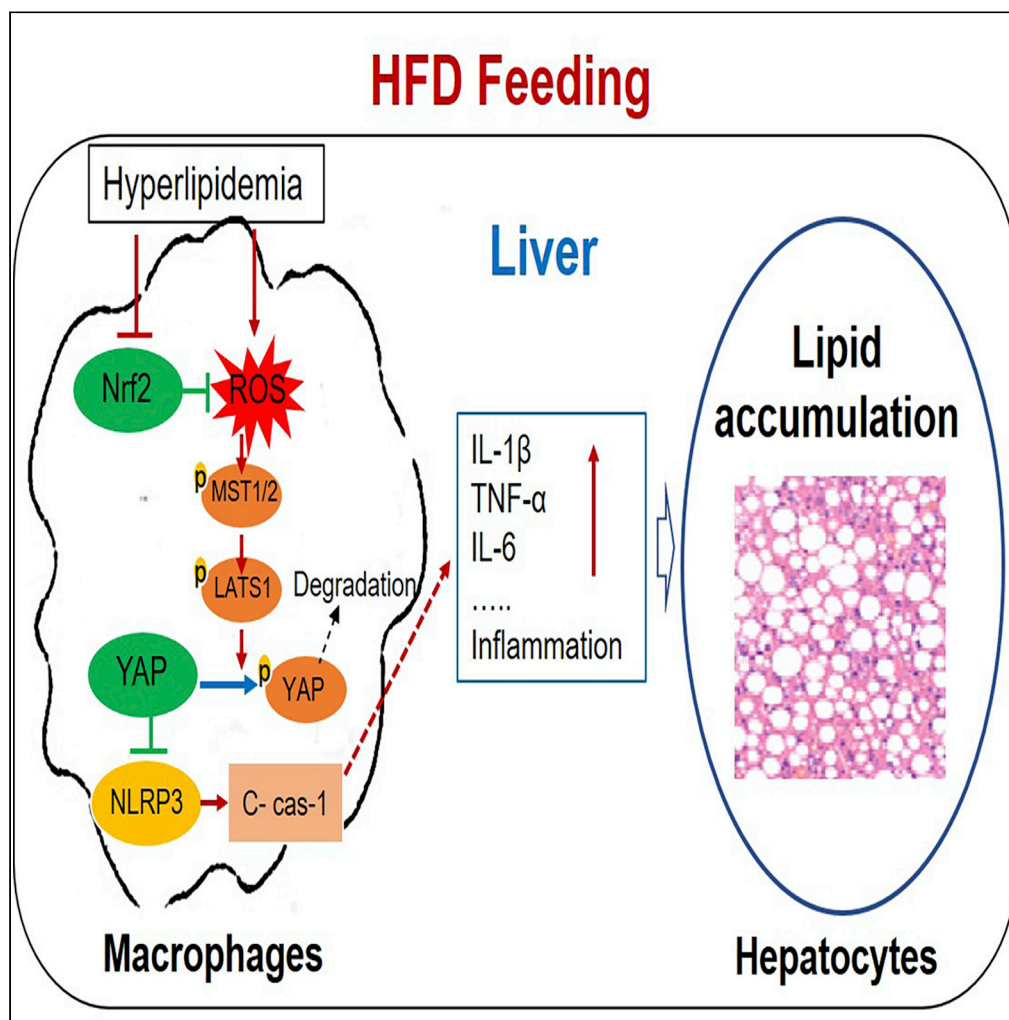


Article

Myeloid Nrf2 deficiency aggravates non-alcoholic steatohepatitis progression by regulating YAP-mediated NLRP3 inflammasome signaling



Peng Wang, Ming Ni, Yizhu Tian, ..., Feng Cheng, Jianhua Rao, Ling Lu

docchengfeng@njmu.edu.cn (F.C.)  
raojh@njmu.edu.cn (J.R.)  
lvling@njmu.edu.cn (L.L.)

Highlights

Kupffer cells Nrf2 was downregulated in both human and mouse NASH livers

Myeloid Nrf2 deficiency aggravates liver steatosis and inflammation in HFD-induced NASH

Nrf2 controls the NLRP3 activation in a ROS-mediated Hippo-YAP signaling manner



## Article

## Myeloid Nrf2 deficiency aggravates non-alcoholic steatohepatitis progression by regulating YAP-mediated NLRP3 inflammasome signaling

Peng Wang,<sup>1,2</sup> Ming Ni,<sup>1,2</sup> Yizhu Tian,<sup>1,2</sup> Hao Wang,<sup>1</sup> Jiannan Qiu,<sup>1</sup> Wenhua You,<sup>1</sup> Song Wei,<sup>1</sup> Yong Shi,<sup>1</sup> Jinren Zhou,<sup>1</sup> Feng Cheng,<sup>1,\*</sup> Jianhua Rao,<sup>1,\*</sup> and Ling Lu<sup>1,3,\*</sup>

## SUMMARY

**Nuclear-erythroid-2-related factor 2 (Nrf2) is involved in the pathogenesis of different liver diseases. Herein, we first demonstrated that Nrf2 expression was diminished in nonalcoholic steatohepatitis (NASH) liver macrophages. In myeloid Nrf2-deficiency mice, aggravated liver steatosis and inflammation in high-fat-diet (HFD)-fed mice were observed compared with the chow-diet group. Moreover, the increasing inflammatory cytokines influenced the lipid metabolism in hepatocytes *in vivo* and *in vitro*. Further study showed Nrf2 regulated reactive-oxygen-species-mediated Hippo-yes-associated protein (YAP) signaling, which in turn modulated the NLRP3 inflammasome activation. Administration of YAP activator also significantly ablated the lipid accumulation and inhibited the NLRP3 activation in the Nrf2 deletion condition both *in vitro* and *in vivo*. Overexpression Nrf2 in liver macrophages effectively alleviated steatohepatitis in wild-type mice fed with an HFD. Our data support that by modulating YAP-mediated NLRP3 inflammasome activity, macrophage Nrf2 slows down NASH progression.**

## INTRODUCTION

Nonalcoholic fatty liver disease (NAFLD), also known as metabolic (dysfunction) associated fatty liver disease, is a disorder in which the patient has an excessive accumulation of fat in the liver without excessive alcohol consumption. NAFLD's clinicopathological spectrum ranges from simple fatty liver to nonalcoholic steatohepatitis (NASH), which involves liver inflammation, eventually leading to cirrhosis, hepatocellular carcinoma, and liver failure (Ibrahim et al., 2018; Younossi et al., 2018; Font-Burgada et al., 2016). Currently, about 22–28% of the global population are suffering from NAFLD. NASH has also become the leading cause of liver transplantation in the clinic (Estes et al., 2018; Friedman et al., 2018). Although NASH's research has become a hot topic in recent years (Patouraux et al., 2017; Musso et al., 2018), there are currently no approved pharmacological therapies for NASH (Friedman et al., 2018). Therefore, we believe obtaining a comprehensive understanding of NASH's cellular mechanism may promote new treatment strategies for this high-incidence disease to relieve global medical burden.

Nuclear-erythroid-2-related factor 2 (NFE2L2/Nrf2) is a basic leucine zipper transcription factor that functions as the primary regulator of cellular protector by inducing anti-inflammatory and antioxidant genes (Dodson et al., 2019; Bellezza et al., 2018). Nrf2 has been implicated to play a critical role in various liver diseases, including acute hepatotoxicity, NASH, alcoholic liver disease, drug-induced liver injury, and so on (Klaassen and Reisman, 2010; Tang et al., 2014; Rao et al., 2015). Under oxidative stress or other external stimuli, Nrf2 can be activated and translocates into the nucleus, where it binds to antioxidant response elements with small Maf proteins to modulate antioxidant genes such as HO-1 and NAD(P)H quinone oxidoreductase 1 at the transcriptional level (Hayes and Dinkova-Kostova, 2014). By upregulating antioxidant genes, Nrf2 could also protect liver against inflammatory response in a reactive-oxygen-species (ROS)-dependent manner (Kobayashi et al., 2016. Qin et al., 2015). However, the cytoprotective functions of Nrf2 make it also to participate in the pathogenesis, progression, and metastasis of multiple cancers even helps tumor develop resistance to chemotherapy, indicating that Nrf2 is a pleiotropic transcription factor in different microenvironments (Rojo de la Vega et al., 2018; Zhou et al., 2019). Interestingly, Nrf2, as a cytoprotective molecular that is elevated under external stimuli, is downregulated in the liver of

<sup>1</sup>Hepatobiliary Center of The First Affiliated Hospital and The Affiliated Cancer Hospital (Jiangsu Cancer Hospital), School of Biomedical Engineering and Informatics, Nanjing Medical University, Research Unit of Liver Transplantation and Transplant Immunology, Chinese Academy of Medical Sciences, 300 Guang Zhou Road, Nanjing, China

<sup>2</sup>These authors contributed equally

<sup>3</sup>Lead contact

\*Correspondence: docchengfeng@njmu.edu.cn (F.C.), raojh@njmu.edu.cn (J.R.), lling@njmu.edu.cn (L.L.)  
<https://doi.org/10.1016/j.isci.2021.102427>



patients with NASH (Azzimato et al., 2020). Therefore, the role of Nrf2 in NASH might be worth exploring in more detail.

Liver-resident macrophages (Kupffer cells) and recruited monocyte-derived macrophages are the major subjects of the liver's innate immune system (Kolios et al., 2006). Although NASH's pathophysiology is multifactorial, innate immune activation is well accepted to play a central role in the initiation and perpetuation of liver inflammation (Rivera et al., 2007; Kazankov et al., 2019). In human livers, increased infiltration of CD68<sup>+</sup> macrophages were observed and correlated with the severity of NAFLD (Park et al., 2007). Accordingly, mouse models of NASH established by the administration of high-fat diet (HFD) feeding also showed elevated macrophage infiltration in the liver compared with controls (Tosello-Trampont et al., 2012). Conversely, the depletion of hepatic macrophages by clodronate liposomes or gadolinium chloride treatment was proven to prevent the progression of steatohepatitis in mouse NASH models (Huang et al., 2010; Neyrinck et al., 2009). Thus, targeting hepatic macrophage may provide new clues for developing appropriate treatment strategies for NASH.

In the present study, we generated myeloid-specific Nrf2-deficient (Nrf2<sup>M-KO</sup>) mice to investigate the contribution of Nrf2 in macrophages during NASH progression. We demonstrated myeloid Nrf2 deficiency aggravated steatohepatitis in mouse NASH models accompanied with elevated inflammatory response and worsening metabolism in a yes-associated protein (YAP)-NLRP3 axis-dependent manner.

## RESULTS

### Nrf2 is downregulated in liver macrophages from mouse NASH models and patients with NAFLD

To determine the role of Nrf2 in macrophages during the pathogenesis of NASH, we first examined Nrf2 expression in liver macrophages from patients with NAFLD and healthy controls, which was confirmed by HE staining (Figure 1A). Figures 1B and 1C show that both Nrf2 mRNA and protein levels were significantly lower in macrophages isolated from NAFLD livers than in normal livers. Subsequently, we used HFD-induced mouse models of NASH to analyze macrophage Nrf2 expression in mice. NASH is induced by HFD feeding evidenced by steatosis and inflammation (Figures 1D and S1). Similarly, the Nrf2 mRNA and protein levels in macrophages were markedly lower in WT mice fed with an HFD than normal chow (NC) for 16 weeks (Figures 1E and 1F). To elucidate the roles/mechanisms of Nrf2 in macrophages during NASH pathogenesis *in vivo*, we generated myeloid-specific Nrf2-deficient mice and then verified the genotypes of Lyz2Cre-Nrf2<sup>FL/FL</sup> mice and the respective control mice, Nrf2<sup>FL/FL</sup> by polymerase chain reaction (PCR) (Figure 1G). Furthermore, we isolated primary hepatocytes and Kupffer cells from the mouse livers, and Western blot results showed a lack of Nrf2 protein in liver macrophages from Nrf2<sup>M-KO</sup> mice (Figure 1H).

### Myeloid-specific Nrf2 deficiency aggravates HFD-induced steatosis

Subsequently, we fed Nrf2<sup>FL/FL</sup> and Nrf2<sup>M-KO</sup> mice an HFD for 16 weeks to establish mouse models of NASH. Interestingly, we observed that the body weight gain and the liver-to-body weight ratio of HFD-fed Nrf2<sup>M-KO</sup> mice were higher than those observed for the control mice (Figures 2A and 2B). The fasting glucose and glucose tolerance of HFD-fed Nrf2<sup>M-KO</sup> mice were worse than Nrf2<sup>FL/FL</sup> mice fed with the same diet (Figures S2B and S2C). Furthermore, macrophage Nrf2 deficiency promotes glucogenesis in the NASH livers (Figure S2C). Hepatic lipid peroxides (thiobarbituric acid reactive substances [TBARS]) and malondialdehyde test kit (TBA microplate method) levels were significantly higher in Nrf2<sup>M-KO</sup> mice than in Nrf2<sup>FL/FL</sup> mice (Figures 2C and S4A). Besides, the glutathione contents and superoxide dismutase activity values were lower in the livers of HFD-fed Nrf2<sup>M-KO</sup> mice than in those of Nrf2<sup>FL/FL</sup> mice (Figure S4A), indicating that the deletion of Nrf2 in macrophages contributed to elevated ROS contents by reducing antioxidant activity. Meanwhile, increased ROS in livers of HFD-fed Nrf2<sup>M-KO</sup> mice compared with that in HFD-fed Nrf2<sup>FL/FL</sup> mice were observed by DHE staining (Figure S2E). Hematoxylin and eosin (HE) staining of liver sections showed greater hepatocyte vacuolation in Nrf2<sup>M-KO</sup> livers than in Nrf2<sup>FL/FL</sup> livers (Figure 2D). Furthermore, HFD-induced steatosis was more severe in liver sections from Nrf2<sup>M-KO</sup> mice than in those from Nrf2<sup>FL/FL</sup> mice, as indicated by increased hepatic lipid accumulation and Oil red O staining (Figures 2E and 2F). The serum alanine aminotransferase (ALT) and aspartate aminotransferase (AST) levels, markers of liver injury, were significantly elevated in Nrf2<sup>M-KO</sup> mice compared with controls (Figure 2G). The aforementioned results indicated that greater lipid accumulation occurred in the livers of Nrf2<sup>M-KO</sup> mice. Next, we examined the expression of lipid metabolism-associated genes in the livers of mice with NASH, the results of which showed that lipogenic transcription factors (FAS, SREBP1c, Pparg, and Fabp4) were upregulated in Nrf2<sup>M-KO</sup> mice compared with

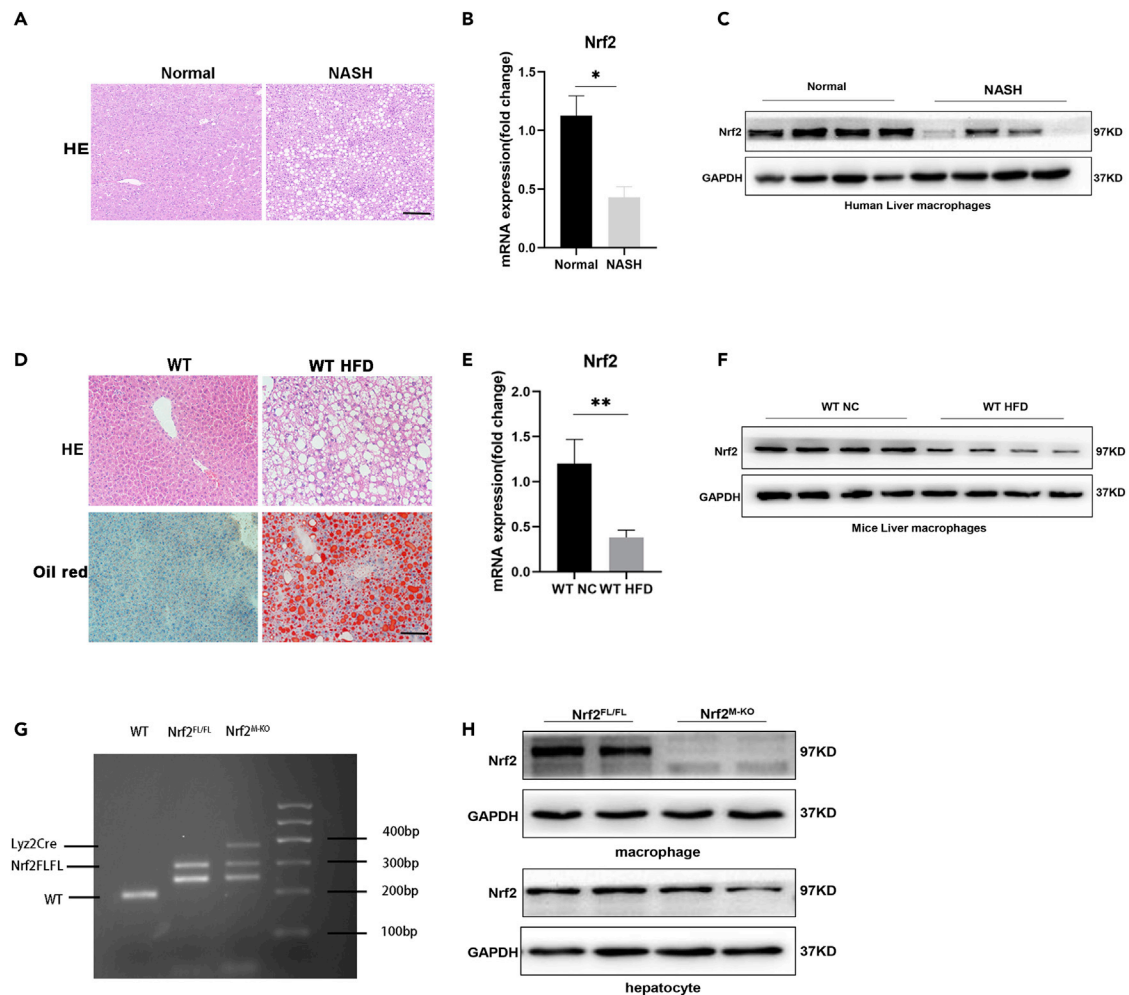


**Figure 1. Nrf2 is downregulated in liver macrophages from mouse NASH models and patients with NAFLD**

Wild-type C57BL/6 mice were fed an HFD or NC diet for 16 weeks.

(A) Representative HE staining of human liver sections (Scale bars, 100 $\mu$ m).

(B) Quantitative reverse transcription PCR analysis of Nrf2 in liver macrophages of patients with NAFLD.

(C) Western blotting analysis of Nrf2 in liver macrophages of patients with NAFLD.

(D) Representative HE and Oil Red O staining of mice NASH liver (Scale bars, 100 $\mu$ m).

(E) Quantitative reverse transcription PCR analysis of Nrf2 in liver macrophages of mouse NASH models.

(F) Western blotting analysis of Nrf2 in liver macrophages of mouse NASH models.

(G) Genotyping analysis of the Ly2Cre-Nrf2<sup>FL/FL</sup> mice and Nrf2<sup>FL/FL</sup> mice.

(H) The Nrf2 expression was detected in hepatocytes and liver macrophages by Western blot assay. N = 4–6. Data are expressed as mean  $\pm$  SD. \*p < 0.05 versus normal group (two-tailed unpaired Student's t test).

Nrf2<sup>FL/FL</sup> mice. In contrast, we noted that the genes involved in modulating lipid  $\beta$ -oxidation (Cpt1a, Cyp4a14, Acadl, and Ppara) were downregulated in Nrf2<sup>M-KO</sup> mice (Figure 2H). These findings suggest that macrophage Nrf2 mitigates the lipid accumulation in the liver upon HFD feeding.

### Myeloid-specific Nrf2 deficiency aggravates HFD-induced liver inflammation and fibrosis

As inflammatory responses play an essential role in the pathophysiological mechanisms of NASH, we next evaluated hepatic inflammation in Nrf2<sup>FL/FL</sup> and Nrf2<sup>M-KO</sup> mice fed an HFD or NC. First, we observed that Nrf2<sup>M-KO</sup> mice showed higher gene expression of proinflammatory cytokines (including tumor necrosis factor [TNF]- $\alpha$ , interleukin [IL]-6, and IL-1 $\beta$ ) than Nrf2<sup>FL/FL</sup> mice, whereas that of anti-inflammatory factors (IL-4 and IL-10) was lower in Nrf2<sup>M-KO</sup> mice fed with HFD than that in Nrf2<sup>FL/FL</sup> mice on the same diet (Figure 3A). Similarly, higher serum TNF- $\alpha$ , IL-6, and IL-1 $\beta$  levels and lower IL-4 and IL-10 protein levels were detected in

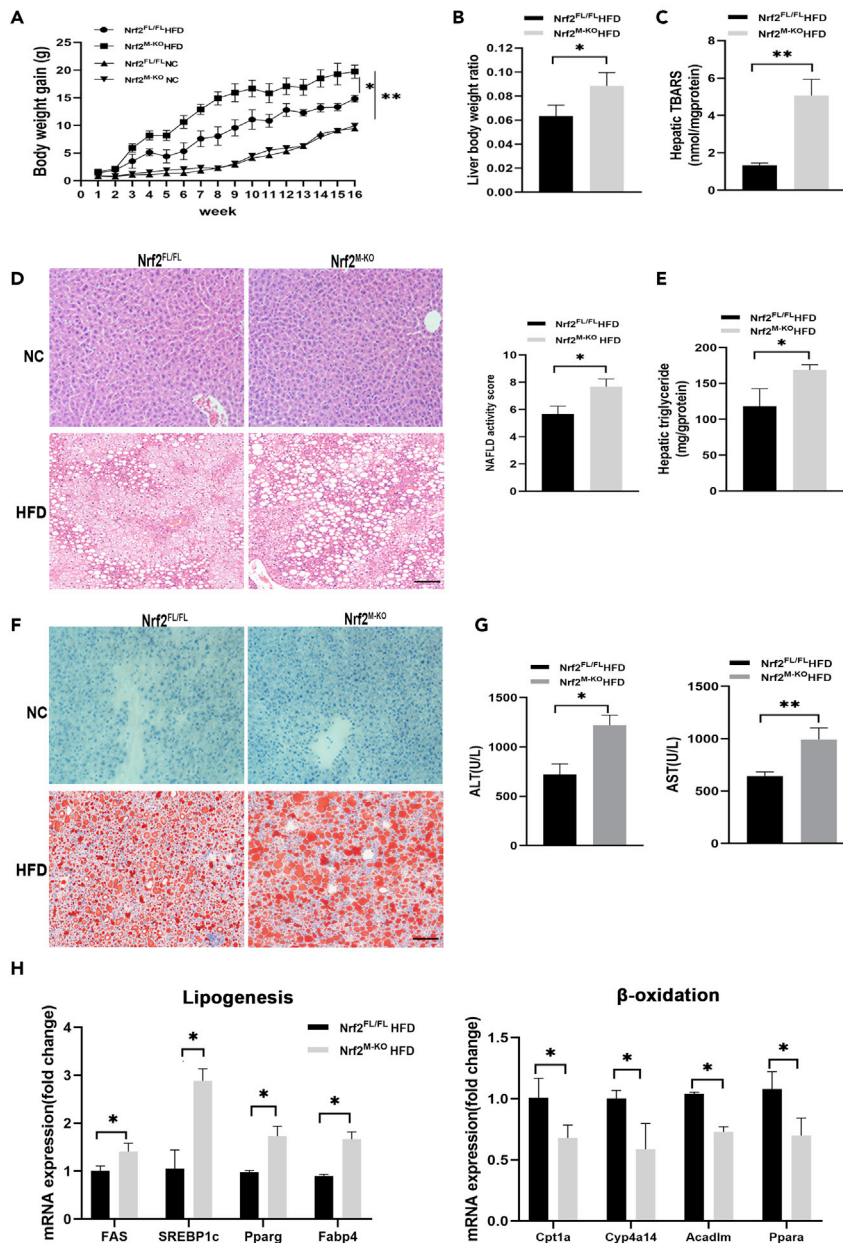


**Figure 2. Myeloid-specific Nrf2 deficiency aggravates HFD-induced NASH in mouse models**

(A) Body weight gain.  
 (B) Liver-to-body weight ratio.  
 (C) Hepatic TBARS.  
 (D) Representative HE staining of liver sections (Scale bars, 100 $\mu$ m) and NAFLD activity scores (NAS).  
 (E) Hepatic triglyceride content.  
 (F) Representative Oil Red O staining of liver section (Scale bars, 100 $\mu$ m).  
 (G) Serum ALT and AST levels.  
 (H) Quantitative reverse transcription PCR analysis of lipogenesis (FAS, SREBP1c, Pparg, Fabp4) and  $\beta$ -oxidation genes (Cpt1a, Cyp4a14, Acad1m, Ppara) in NASH livers. N = 6 mice/group. Data are expressed as mean  $\pm$  SD. \*p < 0.05 versus Nrf2<sup>FL/FL</sup> + HFD group (two-tailed unpaired Student's t test).

Nrf2<sup>M-KO</sup> mice when compared with that in control (Figure 3B). CD11b immunostaining was performed to evaluate the infiltrating monocytes and macrophages in the NASH livers, with the results showing increased CD11b marker levels in Nrf2<sup>M-KO</sup> mice compared with the control mice (Figure 3C). Figure 3D shows that

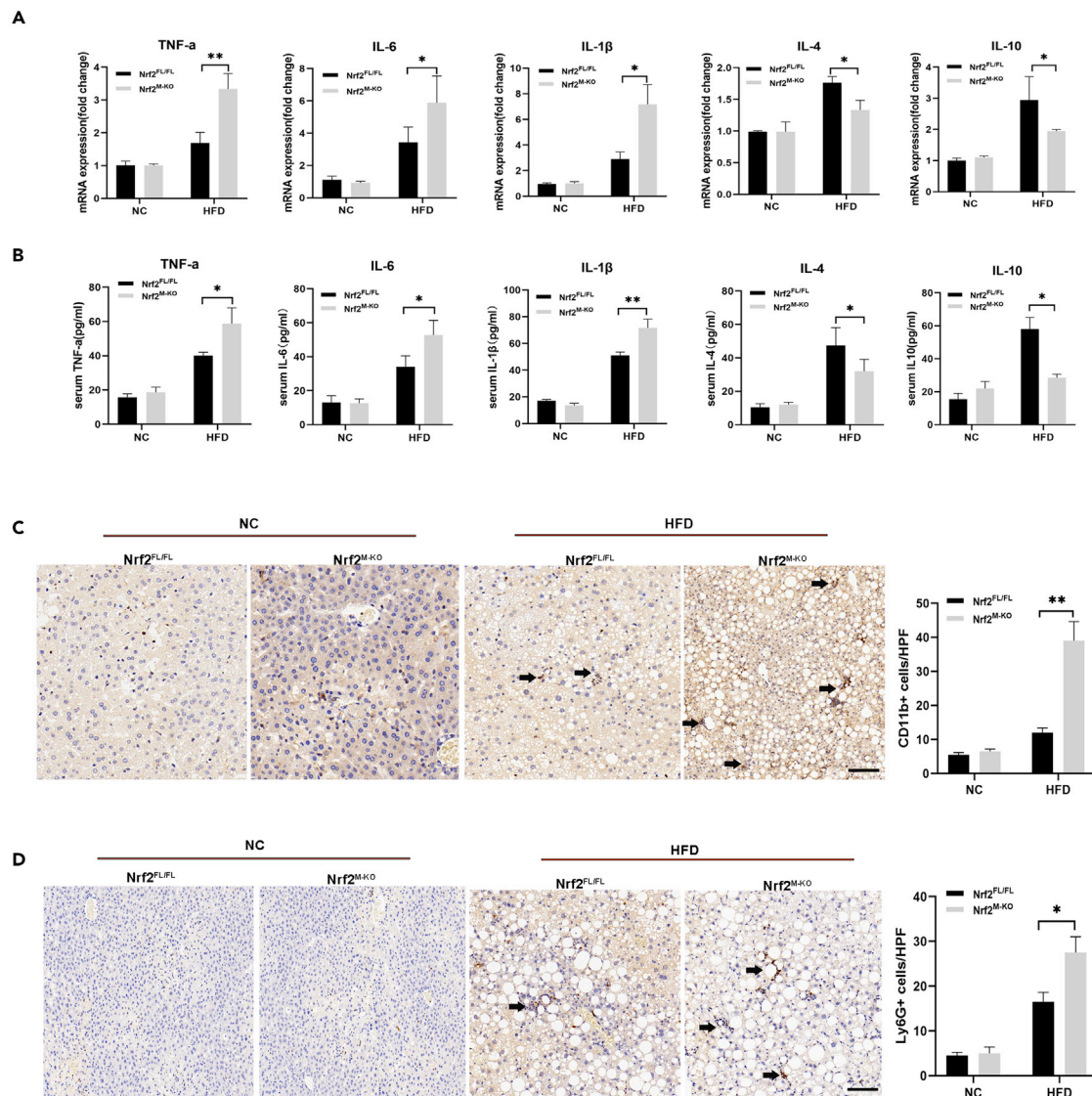


**Figure 3. Myeloid-specific Nrf2 deficiency promotes inflammatory responses in mouse NASH livers**

(A) Quantitative reverse transcription PCR analysis of TNF- $\alpha$ , IL-6, IL-1 $\beta$ , IL-10, and IL-4 in NASH livers.

(B) The serum level of TNF- $\alpha$ , IL-6, IL-1 $\beta$ , IL-10, and IL-4 was detected by ELISA.

(C and D) Immunohistochemical staining of CD11b + macrophages or Ly6G + neutrophils in NASH livers. Quantification of CD11b- or Ly6G-positive cells per high-power field (Scale bars, 50  $\mu$ m). N = 6 mice/group. Data are expressed as mean  $\pm$  SD. \*p < 0.05 versus Nrf2<sup>FL/FL</sup> + HFD group (one-way ANOVA).

more neutrophils were recruited in Nrf2<sup>M-KO</sup> mice fed with HFD compared that in control as indicated by Ly6G immunostaining. The aforementioned data suggest that myeloid-specific Nrf2 deficiency promotes hepatic inflammation by regulating inflammatory factors' secretion and the infiltration of macrophages/neutrophils in NASH. Also, Sirius red and  $\alpha$ -SMA IHC staining revealed the aggravated fibrosis in the liver of Nrf2<sup>M-KO</sup> mice fed with HFD compared with that in the Nrf2<sup>FL/FL</sup> group (Figure S3). Together, these data indicate that myeloid Nrf2 deficiency promotes the development of steatohepatitis.

### Nrf2 deficiency aggravates PA-induced inflammation in BMDMs and influences lipid accumulation in hepatocytes *in vitro*

To determine the effects of Nrf2 on the functions of macrophages *in vitro*, bone-marrow-derived macrophages (BMDMs) were obtained from Nrf2<sup>FL/FL</sup> or Nrf2<sup>M-KO</sup> mice. We used palmitic acid (PA) to mimic a high-fat environment *in vitro*. We detected the gene expression of proinflammatory mediators (TNF- $\alpha$ ,

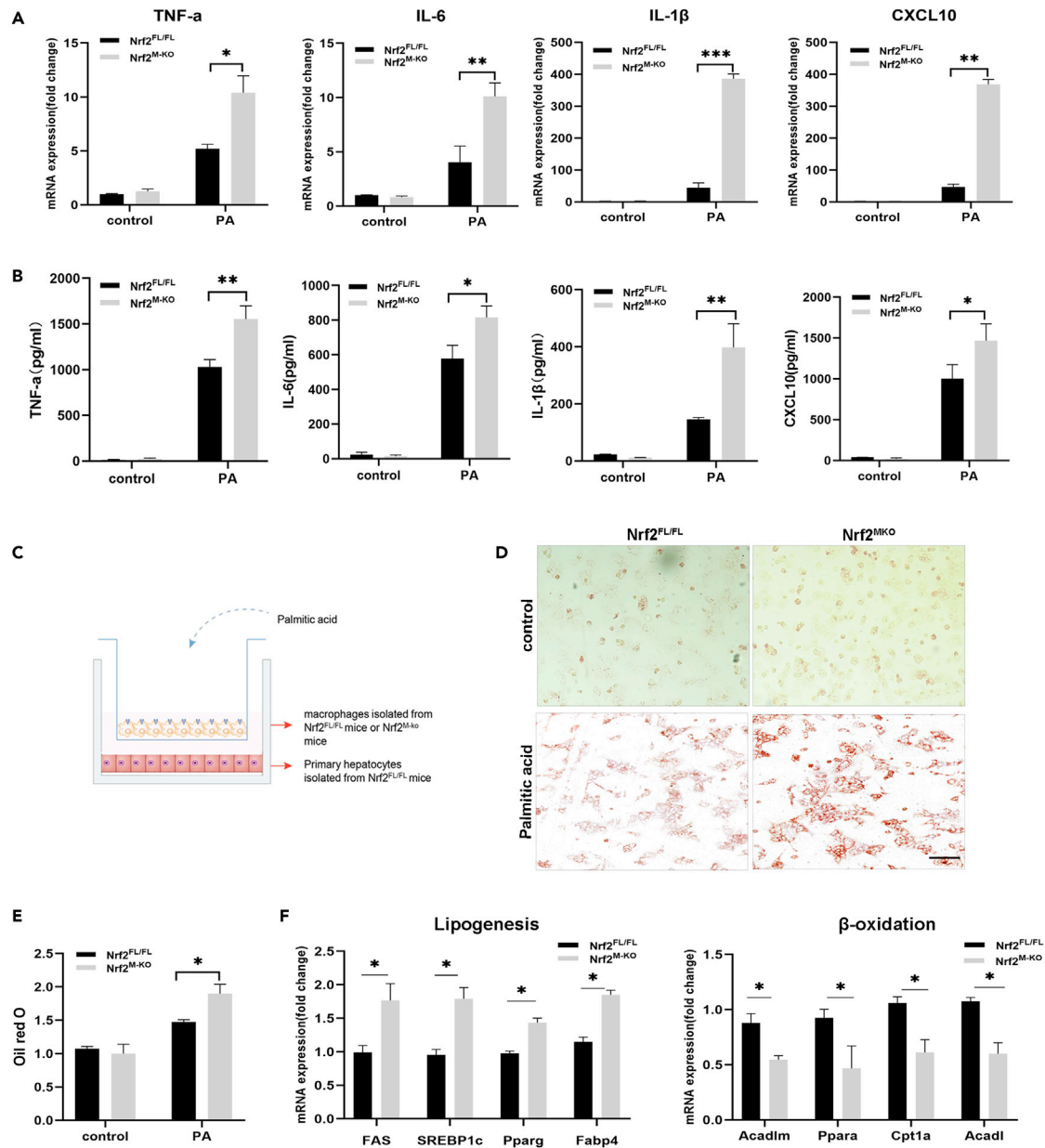


**Figure 4. Nrf2 deficiency aggravates PA-induced inflammation in BMDMs and influences lipid accumulation in hepatocytes *in vitro***

BMDMs were generated from the bone marrow of Nrf2<sup>FL/FL</sup> or Nrf2<sup>M-KO</sup> mice and treated with palmitic acid 200μm or 5% BSA (bovine albumin) for 24 h. (A) Quantitative reverse transcription PCR analysis of TNF-α, IL-6, IL-1β, and CXCL10 in BMDMs treated with PA.

(B) Enzyme-linked immunosorbent assay of TNF-α, IL-6, IL-1β, and CXCL10 in cell culture supernatants.

(C) Schematic showing that the macrophages (10<sup>5</sup>) isolated from bone marrow of Nrf2<sup>FL/FL</sup> or Nrf2<sup>M-KO</sup> mice were cocultured with primary Nrf2<sup>FL/FL</sup> hepatocytes (5 × 10<sup>5</sup>) with or without PA.

(D) Oil Red O staining of palmitic-acid-treated hepatocytes cocultured with BMDMs (Scale bars, 100μm magnification).

(E) Semiquantitate analysis of Oil Red O staining of palmitic-acid-treated hepatocytes.

(F) The mRNA levels of lipogenesis genes (FAS, SREBP1c, Pparg, Fabp4) and β-oxidation genes (Cpt1a, Cyp4a14, Acadlm, Ppara) in hepatocytes cocultured with BMDMs. N = 4. Data are expressed as mean ± SD. \*p < 0.05 versus Nrf2<sup>FL/FL</sup> + PA group (one-way ANOVA and two-tailed unpaired Student's t test).

IL-6, IL-1β, and CXCL10), the levels of which were higher in Nrf2-deficient BMDMs than in control BMDMs (Figure 4A). Consistent with this result, the supernatant levels of TNF-α, IL-6, IL-1β, and CXCL10 were also higher in Nrf2-deficient BMDMs than in WT BMDMs (Figure 4B). To investigate whether macrophage Nrf2 deficiency exacerbates hepatocytes' lipid metabolism *in vitro*, primary hepatocytes isolated from Nrf2<sup>FL/FL</sup>

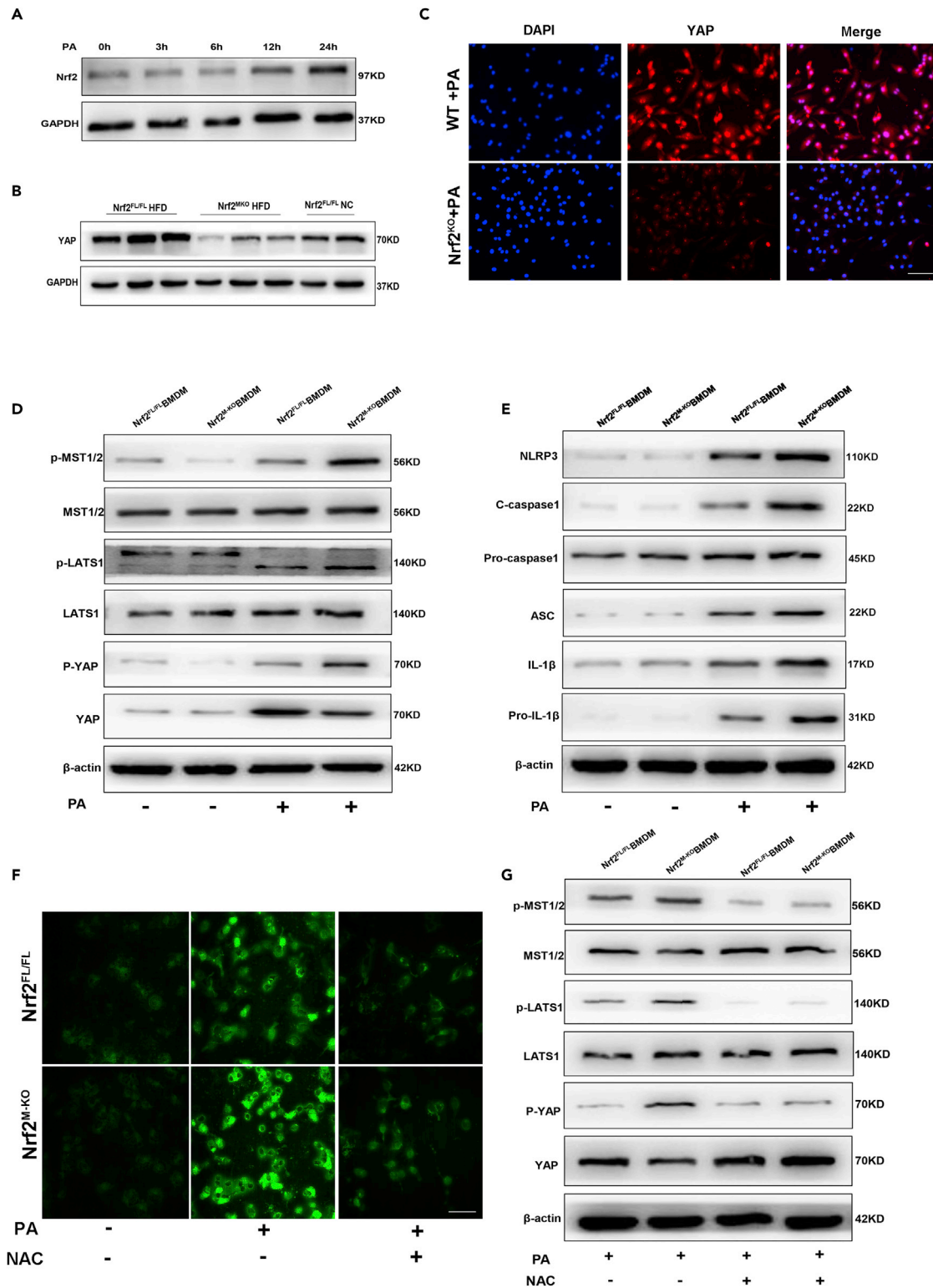


**Figure 5. Nrf2 attenuates inflammation in PA-induced macrophages by enhancing YAP activation**

(A) The Nrf2 protein levels in primary macrophages treated with 200 μM PA.

(B) The YAP protein expression in liver of Nrf2<sup>FL/FL</sup> or Nrf2<sup>M<sup>-</sup>KO</sup> mice with NASH.

(C) Immunofluorescence staining of YAP in different groups of BMDMs (Scale bars, 20 μm).

**Figure 5. Continued**

(D) Western blotting analysis of p-MST1/2, MST1/2, p-LATS1, LATS1, p-YAP, YAP in different groups of BMDMs.

(E) Western blotting analysis of macrophages NLRP3, cleaved caspase-1, procaspase-1, ASC, IL-1 $\beta$ , pro-IL-1 $\beta$ .

(F) Immunofluorescence analysis of ROS in different groups of BMDMs (Scale bars, 100 $\mu$ m).

(G) Western blotting analysis of p-MST1/2, MST1/2, p-LATS1, LATS1, p-YAP, YAP in Nrf2<sup>FL/FL</sup> and Nrf2<sup>M-KO</sup> BMDMs coupled with NAC (5 $\mu$ M, 24 h) or not. All results are representative of three independent Experiments.

mice were cocultured with BMDMs isolated from Nrf2<sup>FL/FL</sup> or Nrf2<sup>M-KO</sup> mice in PA medium using a Transwell system (Figure 4C). Then, we found Nrf2-deficient BMDMs promoted increased lipid accumulation in primary hepatocytes compared with that observed in cocultures with WT BMDMs, as indicated by ORO staining results (Figures 4D and 4E). To further confirm the impact of macrophages on steatosis changes in hepatocytes, we also assessed the expression of lipogenesis and  $\beta$ -oxidation genes in hepatocytes cocultured with Nrf2<sup>FL/FL</sup> or Nrf2<sup>M-KO</sup> BMDMs. Compared with Nrf2<sup>FL/FL</sup> BMDMs, Nrf2<sup>M-KO</sup> BMDMs increased lipogenesis genes expression (FAS, SREBP1c, Pparg, and Fabp4) in hepatocytes *in vitro* (Figure 4F). Conversely, the expression of  $\beta$ -oxidation genes (Cpt1a, Cyp4a14, Acadlm, and Ppara) was lower in hepatocytes cocultured with Nrf2<sup>M-KO</sup> BMDMs compared with that observed in the control cells (Figure 4F). These results demonstrated that Nrf2 deficiency promoted PA-treated BMDMs to secrete inflammatory factors, which subsequently exacerbated lipid accumulation in primary hepatocytes.

**Nrf2 attenuates inflammation in PA-induced macrophages by enhancing YAP activation**

To further investigate the mechanism by which macrophage Nrf2 regulates steatohepatitis, Nrf2<sup>FL/FL</sup> BMDMs were treated with PA for 0 to 24 h. In contrast to the Nrf2 expression observed in mice's liver macrophages with NASH, the Nrf2 protein levels gradually increased in PA-treated macrophages over time (Figure 5A). The previous studies suggested that silencing Nrf2 or glutathione depletion can reduce YAP expression in cancer cells (Cucci et al., 2020; Wu et al., 2013). Surprisingly, YAP protein expression was also downregulated in NASH livers from Nrf2<sup>M-KO</sup> mice compared with that in control (Figure 5B). Interestingly, Figure 5C shows that nuclear YAP expression was higher in Nrf2<sup>FL/FL</sup> BMDMs after PA treatment than in Nrf2<sup>M-KO</sup> BMDMs. The YAP protein expression was also decreased in PA-treated Nrf2<sup>M-KO</sup> BMDMs than in the control cells. In addition, PA treatment promoted YAP's nuclear translocation in macrophages evidenced by increased nuclear YAP expression (Figure S5A). As shown in Figure 5D, Nrf2<sup>M-KO</sup> BMDMs exhibited increased phosphorylation of MST1/2 (p-MST1/2), LATS1 (p-LATS1), and YAP (p-YAP) compared with Nrf2<sup>FL/FL</sup> BMDMs. These data indicate that Nrf2 deficiency activates Hippo signaling, promotes YAP degradation, and reduces nuclear YAP levels in macrophages treated with PA. Hippo signaling controls NLRP3 inflammasome function through the YAP- $\beta$ -catenin complex during liver ischemic reperfusion injury (Li et al., 2019). Therefore, we compared NLRP3 inflammasome activation in Nrf2<sup>FL/FL</sup> or Nrf2<sup>M-KO</sup> BMDMs after PA treatment. The results showed that NLRP3, ASC, cleaved caspase-1, and mature IL-1 $\beta$  levels were significantly higher in Nrf2<sup>M-KO</sup> BMDMs exposed to PA than was observed in the control cells (Figure 5E). Previous studies have demonstrated that Nrf2 modulates oxidative stress by regulating antioxidant gene expression (Dodson et al., 2019; Bellezza et al., 2018). In addition, the ROS released from phagosome or mitochondria recruits MST1/2 and subsequently promoted the phosphorylation of MST1/2 (Wang et al., 2019). Therefore, we hypothesized that Nrf2 regulates the Hippo signaling in an ROS-dependent manner. ROS production was significantly increased in PA-treated Nrf2<sup>M-KO</sup> BMDMs, as indicated by H<sub>2</sub>DCFDA staining, whereas pretreatment with the essential ROS scavenger N-acetylcysteine (NAC) significantly decreased ROS accumulation (Figure 5F). Then, the effects of ROS on Hippo signaling were investigated in macrophages treated with NAC. The results presented in Figure 5G show that NAC recovered YAP activation by decreasing p-MST1/2, p-LATS1, and p-YAP levels. We further detected the XBP1 and  $\beta$ -catenin expression in the PA-treated macrophages. The results showed that Nrf2 deficiency increased the XBP1 expression but downregulated the  $\beta$ -catenin protein levels (Figure S5B). These results suggest that Nrf2 deficiency aggravates PA-induced inflammation by promoting Hippo signaling in an ROS-dependent manner, which in turn regulates NLRP3 activation in a YAP/ $\beta$ -catenin/XBP1-dependent manner.

**YAP activator ameliorates inflammation of PA-induced Nrf2<sup>M-KO</sup> BMDMs and hepatocytes lipid accumulation**

To further explore the cross talk between the YAP and Nrf2, we used the YAP agonist 1-oleoyl lysophosphatidic acid (LPA) to restore YAP activity. As shown in Figures 6A and 6B, YAP protein expression was rescued in Nrf2<sup>M-KO</sup> BMDMs compared with that without LPA treatment. Intriguingly, YAP activation significantly attenuated inflammation in Nrf2<sup>M-KO</sup> BMDMs after PA exposure (Figures 6C and 6D). Furthermore,

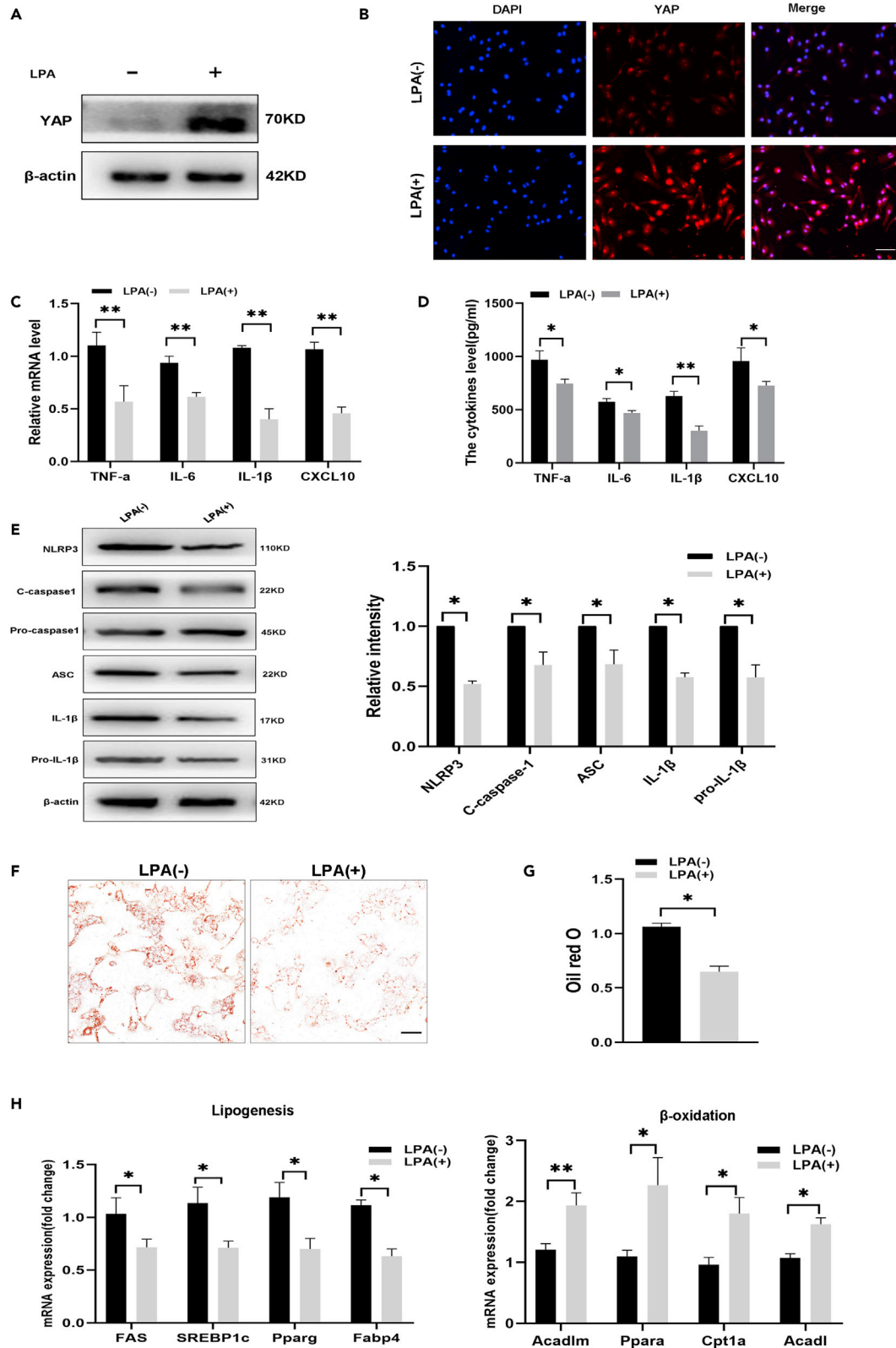


### Figure 6. YAP activator ameliorates inflammation of PA-induced Nrf2<sup>M-KO</sup> BMDMs and hepatocytes lipid accumulation

The Nrf2<sup>M-KO</sup> BMDMs were treated with LPA (10μm) for YAP activation.

(A) Western blotting analysis of YAP in Nrf2<sup>M-KO</sup> BMDMs.

(B) The immunofluorescence staining of YAP in Nrf2<sup>M-KO</sup> BMDMs (Scale bars, 20μm).

(C) Quantitative reverse transcription PCR analysis of TNF-α, IL-6, IL-1β, and CXCL10 in BMDMs.

(D) Enzyme-linked immunosorbent assay of TNF-α, IL-6, IL-1β, and CXCL10 in cell culture supernatants.

(E) Western blotting analysis of macrophages NLRP3, ASC, cleaved caspase-1, procaspase-1, ASC, IL-1β, pro-IL-1β.

(F) Oil Red O staining of palmitic-acid-treated hepatocytes cocultured with Nrf2<sup>M-KO</sup> BMDMs supplemented with LPA or not (Scale bars, 100μm).

(G) Semiquantitative analysis of Oil Red O staining of palmitic-acid-treated hepatocytes.

(H) The mRNA levels of lipogenesis genes (FAS, SREBP1c, Pparg, Fabp4) and β-oxidation genes (Cpt1a, Cyp4a14, Acadm, Ppara) in hepatocytes. N = 4. Data are expressed as mean ± SD. \*p < 0.05 versus Nrf2<sup>M-KO</sup> BMDMs + LPA(-) group (two-tailed unpaired Student's t test).

Figure 6E shows that YAP restoration effectively inhibited NLRP3 inflammation activation, as indicated by decreased protein expression of NLRP3, ASC, cleaved caspase-1, and IL-1β. Then, we evaluated the effects of YAP restoration in Nrf2<sup>M-KO</sup> BMDMs on lipid accumulation in hepatocytes. Notably, the PA-containing coculture system supplemented with LPA resulted in lower lipid accumulation in hepatocytes, as indicated by ORO staining (Figures 6F and 6G), further confirmed by gene expression lipid metabolism (Figure 6H). LPA also increased YAP activation in hepatocytes. We checked the lipid accumulation of PA-treated hepatocytes with or without LPA treatment (Figure S4B), which showed no significant change in lipid accumulation of hepatocytes *in vitro*. The aforementioned results show that macrophage Nrf2 regulates NLRP3 inflammation activation by stabilizing YAP function, ultimately influencing lipid metabolism in hepatocytes.

### YAP activator administration alleviates HFD-induced steatohepatitis in Nrf2<sup>M-KO</sup> mice

To further evaluate the cross talk between YAP and Nrf2 in NASH, Nrf2<sup>M-KO</sup> mice were infused with LPA (0.8 μmol/kg, i.v.) for 4 weeks after being fed an HFD for 8 weeks (Figure 7A). LPA significantly improved liver injury marker levels, as shown in Figure 7B, and HE and ORO staining showed lower steatosis and inflammation in HFD-fed Nrf2<sup>M-KO</sup> mice treated with LPA than in those treated with PBS (Figure 7C). Accordingly, decreased lipid accumulation was observed in the LPA treatment group, as indicated by TG quantification assay results (Figure 7D). Figure 7E shows that LPA ameliorated lipid peroxidation in the livers of Nrf2<sup>M-KO</sup> mice with NASH. To evaluate the effects of LPA on liver macrophages, we isolated Kupffer cells (KCs) from Nrf2<sup>M-KO</sup> mice treated with or without LPA. Western blot results revealed increased YAP activation in the LPA-treated mice compared with the controls (Figure 7F). Gene expression of proinflammatory cytokines was significantly decreased in the isolated KCs from HFD-fed Nrf2<sup>M-KO</sup> mice treated with LPA compared with the controls (Figure 7G). In addition, the culture supernatant levels of TNF-α, IL-6, IL-1β, and CXCL10 showed similar results as the gene expression findings (Figure 7I). Furthermore, YAP activation inhibited NLRP3 inflammasome function in KCs isolated from Nrf2<sup>M-KO</sup> mice after HFD exposure, as evidenced by Figure 7H. These results showed that YAP activation in Nrf2<sup>M-KO</sup> mice with NASH alleviates steatohepatitis progression by regulating NLRP3 inflammation.

### Nrf2 overexpression in macrophages alleviates HFD-diet-induced steatohepatitis

To further assess whether Nrf2 overexpression in macrophages attenuates NASH *in vivo*, we used an adeno-associated virus (AAV) to overexpress Nrf2 (Figure 8A). As the synthetic promoter, SP146-C1 showed higher specificity and efficacy in RAW264.7 cell lines than in nonmacrophage cell lines (Kang et al., 2014), we selected the unique sequence to generate a construct expressing Nrf2 from a macrophage-specific promoter. The Nrf2 protein levels in liver macrophages isolated from WT mice treated with AAV-SP-Nrf2 were higher than those observed in control mice (Figure 8B). Nrf2 overexpression significantly improved the signs of liver injury (Figures 8C–8E). Furthermore, Nrf2 overexpression alleviated proinflammatory cytokine production in the liver (Figures 8F and 8G). Nrf2 overexpression decreased p-MST1/2, p-LATS1, and p-YAP levels but augmented YAP expression in Kupffer cells isolated from mice with NASH (Figure 8H). In addition, NLRP3 and cleaved caspase-1 levels were also decreased in the Nrf2-overexpression group (Figure 8I). Finally, WT BMDMs infected with lenti-Nrf2 showed decreased IL-1β production, whereas the YAP inhibitor verteporfin abrogated the effect of Nrf2 overexpression (Figure 8J). These results collectively indicate that Nrf2 inhibits macrophages' inflammatory response by regulating YAP-mediated NLRP3 activation.

## DISCUSSION

Owing to unhealthy diet habits, NAFLD has become a worldwide health issue (Ibrahim et al., 2018; Younossi et al., 2018; Font-Burgada et al., 2016). In some cases, NAFLD may even develop into NASH—a form of NAFLD in which hepatitis is involved. The metabolic disorder of liver parenchymal cells plays a major

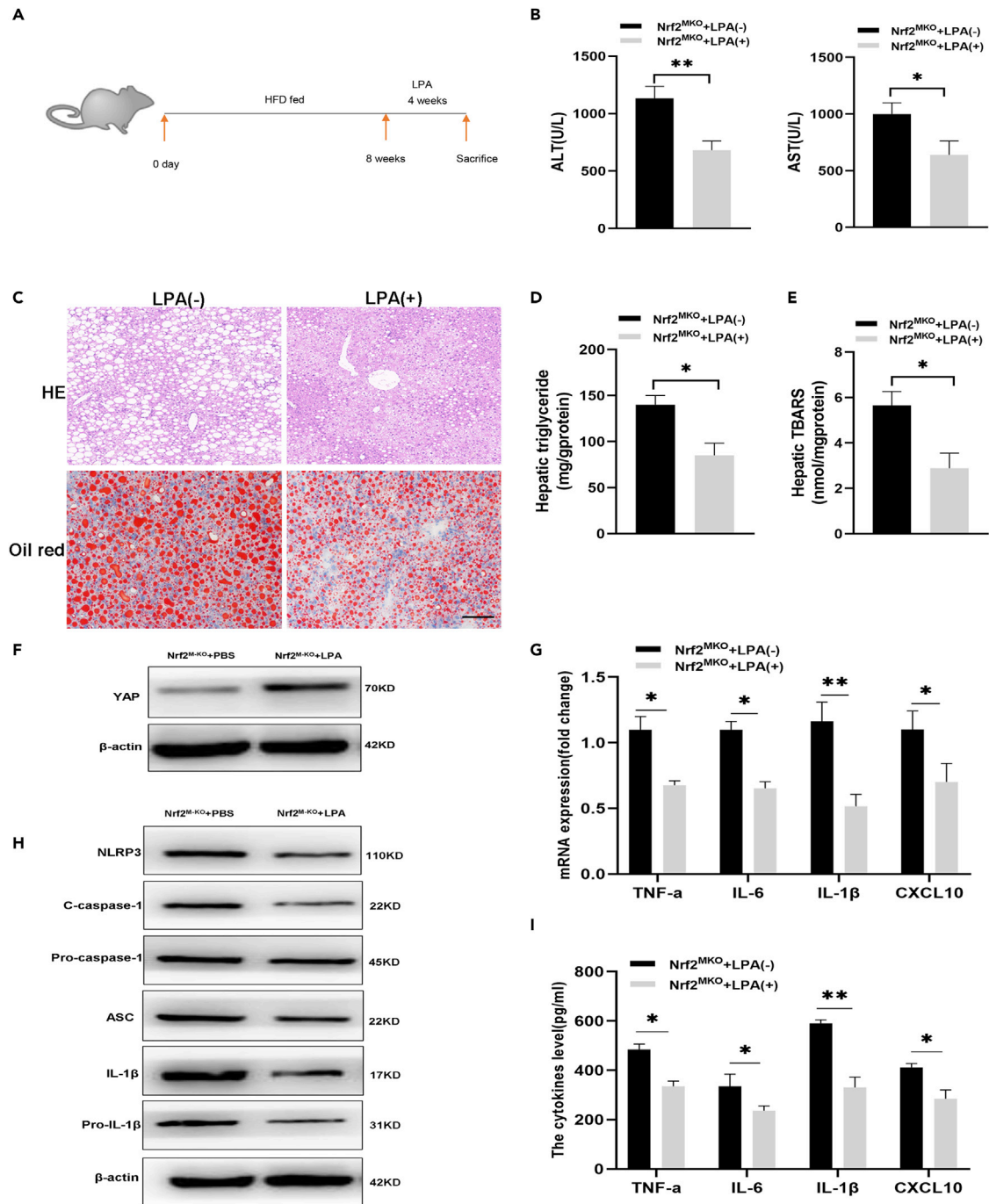


**Figure 7. YAP activator administration alleviates HFD-induced steatohepatitis in  $Nrf2^{M-KO}$  mice**

(A) Schematic showing that  $Nrf2^{M-KO}$  mice were fed with an HFD for 12 weeks. After 8 weeks of HFD diet feeding, LPA was administered per 3 days at doses of 0.8μmol/kg by tail vein injection.

(B) Serum ALT and AST levels.

(C) Representative HE staining and Oil Red O staining of liver sections (Scale bars, 100μm).

(D and E) Hepatic TBARS and triglyceride content.

(F) The protein level of YAP in the KCs isolated from liver tissues of  $Nrf2^{M-KO}$  mice treated with LPA after HFD exposure.

(G) The mRNA level of proinflammatory genes in the KCs isolated from livers was measured by RT-PCR.

(H) Western blot analysis of macrophages NLRP3, cleaved caspase-1, procaspase-1, ASC, IL-1β, pro-IL-1β.

**Figure 7. Continued**

(I) The cytokines level of TNF- $\alpha$ , IL-6, IL-1 $\beta$ , and CXCL10 in cell culture supernatants were measured by ELISA. The isolated KCs from different experimental groups were cultured for 6 h before further examination. N = 6 mice/group. All results are representative of three independent Experiments. Data are expressed as mean  $\pm$  SD. \*p < 0.05 versus Nrf2<sup>M-KO</sup>mice + LPA(-) group (two-tailed unpaired Student's t test).

role in this process. However, in recent years, the importance of the immune response in NAFLD progression to NASH has gradually emerged (Rivera et al., 2007; Kazankov et al., 2019). Therefore, it is worth noting to investigate the role of macrophages—the essential part of innate immune system in the pathogenesis of NASH.

The transcription factor Nrf2 is considered to be a “master switch” of intracellular redox homeostasis, regulating cellular resistance against oxidative stress (Ma, 2013). A previous study showed that Nrf2-deficient liver grafts were susceptible to IR-mediated damage (Ke et al., 2013). Herein, we observed decreased Nrf2 levels in liver macrophages from humans or mice with NASH, which was consistent with the previous study reporting that Nrf2 were decreased in the liver of mice with obesity-induced insulin resistance (Azzimato et al., 2020). Subsequently, we generated myeloid-specific Nrf2-deficient mice to investigate the role of macrophage Nrf2 in NASH's pathogenesis. Interestingly, the body weight of HFD-fed Nrf2<sup>M-KO</sup> mice elevated compared with HFD-fed Nrf2<sup>FL/FL</sup> mice, whereas no difference of food intake was observed between these two groups, indicating that altered mice body weight by myeloid Nrf2 deficiency was not related with food intake. In addition, the results show that HFD-fed Nrf2<sup>M-KO</sup> mice suffered from more severe steatohepatitis than the control mice. In addition, myeloid-specific Nrf2 deficiency exacerbated hepatic inflammation by inducing excessive proinflammatory cytokines production and promoting the migration of macrophages and neutrophils. Consistent with the robust inflammatory response in the livers of Nrf2<sup>M-KO</sup> mice exposed to an HFD, the levels of proinflammatory cytokines also elevated in Nrf2 deficient macrophages treated with PA compared with that in control. Furthermore, the upregulated lipogenic genes were observed in Nrf2<sup>M-KO</sup> mice with NASH, whereas lipolytic genes were downregulated, indicating that myeloid Nrf2 deficiency influenced hepatic lipid metabolism in mouse NASH models. In parallel, the coculture system assays demonstrated that Nrf2-deficient macrophages exacerbate lipid accumulation in hepatocytes *in vitro*. Compelling evidence has shown that proinflammatory factors participate in modulating lipid metabolism in hepatocytes. For instance, TNF- $\alpha$  and IL-1 $\beta$  can reduce the mRNA levels of PPAR $\alpha$ , which contributes to a decrease of peroxisomal  $\beta$ -oxidation (Beier et al., 1992, 1997; Stienstra et al., 2010). Furthermore, recombinant IL-10 treatment was shown to attenuate lipid accumulation and inflammatory and apoptotic signaling in hepatocytes (Han et al., 2017). Our data demonstrated that myeloid Nrf2 deficiency lead to lipid metabolism disorders by inducing the production of proinflammatory cytokines.

It has been reported that Nrf2 regulates inflammatory response mainly by clearance of ROS, which is a potent activator of several inflammatory pathways. However, the exact mechanism remains to be revealed. Previous studies have shown that the Hippo signaling pathway is a major regulator of tissue growth and organ size and that YAP, key downstream effectors of the Hippo pathway, can regulate cell proliferation, apoptosis, and fate (Varelas, 2017; Basu et al., 2003). Although Hippo signaling has multiple roles in different contexts and microenvironments, drug-induced YAP activation in the liver can alleviate hepatic ischemia-reperfusion injury in mice by inhibiting the innate inflammatory response, necrosis/apoptosis and oxidative stress (Liu et al., 2019; Zhou et al., 2018). By interacting with  $\beta$ -catenin, YAP can modulate XBP1 expression, which in turn regulates NLRP3 activation (Li et al., 2019). The cross talk between Nrf2 and YAP has been shown to facilitate antioxidant activity in bladder cancer cells (Cucci et al., 2020). Consistent with these studies, YAP activation by LPA protects the liver against NASH. Intriguingly, we observed decreased YAP protein levels and increased ROS accumulation in the livers of HFD-fed Nrf2<sup>M-KO</sup> mice. The same trend was observed in Nrf2<sup>M-KO</sup> BMDMs treated with PA. ROS production was significantly increased in Nrf2<sup>M-KO</sup> BMDMs after PA treatment, as was previously described (Kobayashi et al., 2016). ROS overproduction has been proven to recruit the MST1/2 from the cytosol to the mitochondrial membrane and promote MST1/2 phosphorylation (Wang et al., 2019). In present study, we noted that the ROS accumulation caused by Nrf2 deficiency promoted the phosphorylation of MST1/2 and LATS1 accompanied with elevated YAP phosphorylation in macrophages. What is more, the ROS scavenger NAC reversed YAP activation in Nrf2<sup>M-KO</sup> BMDMs, providing stronger evidence that Nrf2 modulates Hippo signaling in a ROS-dependent manner. Our data collectively demonstrated that Nrf2 modulates Hippo signaling by controlling ROS production in the murine NASH model.

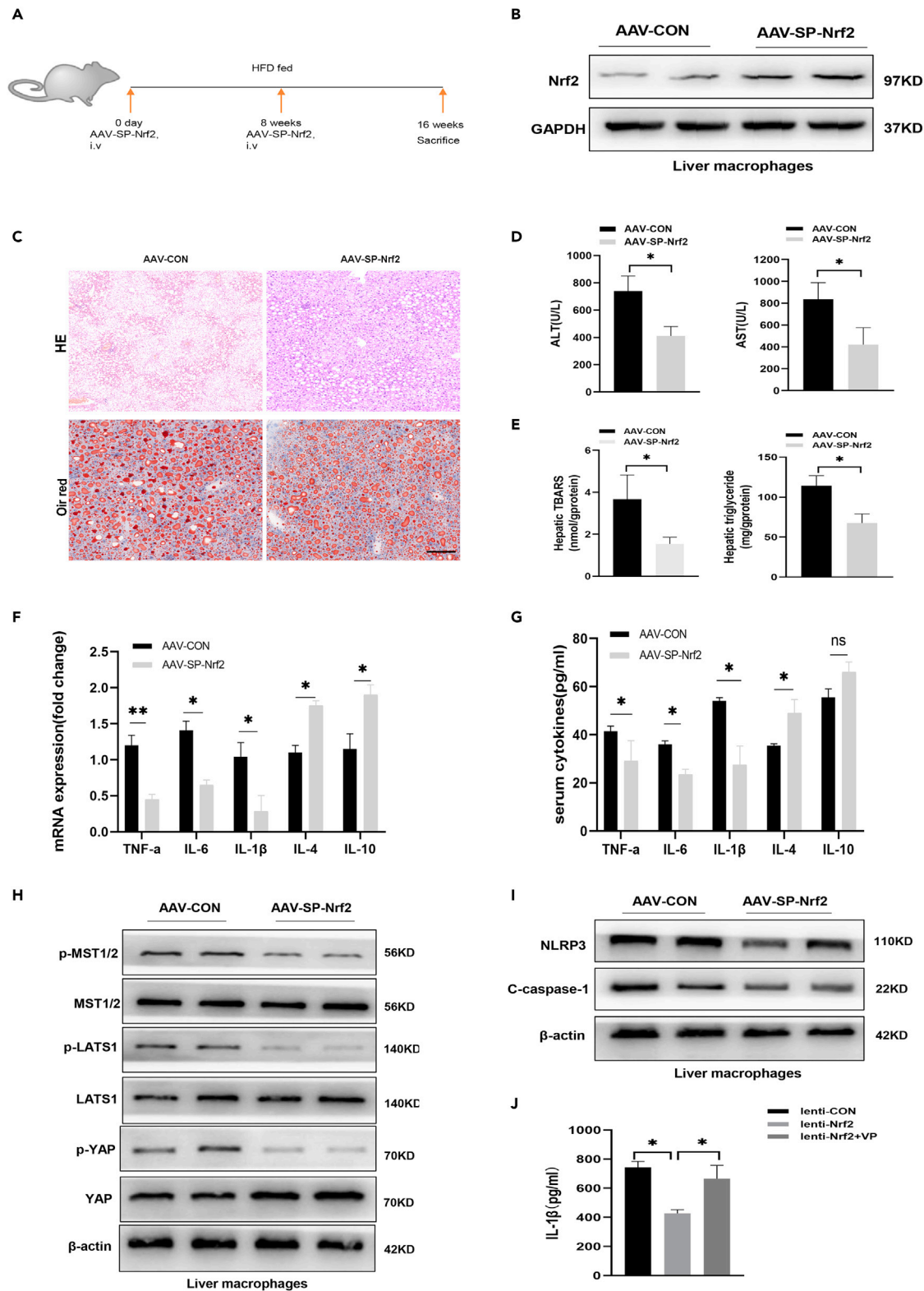


**Figure 8. Nrf2 overexpression in macrophages alleviates HFD-diet-induced steatohepatitis**

(A) Schematic showing that the WT mice were fed with HFD for 16 weeks. The AAV-SP-Nrf2 or AAV-CON was administrated at the beginning and in the middle of 16-week high-fat-diet feeding.

**Figure 8. Continued**

- (B) The protein level of Nrf2 in the KCs isolated from liver tissues of WT mice treated with AAV-SP-Nrf2 (representative of three experiments).  
 (C) Representative HE Staining and Oil Red O staining of liver sections (Scale bars, 100 $\mu$ m).  
 (D) Serum ALT and AST levels.  
 (E) Hepatic TBARS and triglyceride content.  
 (F) Relative hepatic mRNA levels of TNF- $\alpha$ , IL-6, IL-1 $\beta$ , IL-10, and IL-4 by quantitative real-time PCR.  
 (G) The serum level of TNF- $\alpha$ , IL-6, IL-1 $\beta$ , IL-10, and IL-4 was detected by ELISA.  
 (H and I) Western blot analysis of p-MST1/2, MST1/2, p-LATS1, LATS1, p-YAP, YAP, NLRP3, C-caspase-1 in Kupffer cells obtained from NASH livers (representative of three experiments).  
 (J) The IL-1 $\beta$  cytokine level in WT BMDMs (representative of three experiments). The isolated KCs from different experimental groups were cultured for 6 h before further examination. N = 6 mice/group. Data are expressed as mean  $\pm$  SD. \*p < 0.05 versus AAV-CON group (two-tailed unpaired Student's t test).

The NLRP3 inflammasome is a multiprotein complex that can activate caspase-1 and release IL-1 $\beta$  and IL-18 (Szabo and Csak, 2012). A previous study suggested that NLRP3 plays a proinflammatory role in KCs during NASH progression by increasing IL-1 $\beta$  secretion (Cai et al., 2017). Furthermore, another study demonstrated that treatment with sulforaphane, a pharmacological inhibitor of NLRP3 inflammasomes, could alleviate steatohepatitis in mouse NASH models (Yang et al., 2016). Overall, these studies' results demonstrate that NLRP3 inflammasome activation plays a crucial role in the development of NASH. We observed that Nrf2 deficiency promoted NLRP3 activation in macrophages. However, the restoration of YAP expression in Nrf2<sup>M-KO</sup> BMDMs could counteract Nrf2-deficiency-induced NLRP3 inflammasome activation and inflammatory responses in macrophages *in vitro*. Furthermore, the restoration of YAP expression in Nrf2<sup>M-KO</sup> mice with NASH by LPA treatment alleviated steatohepatitis and was accompanied by decreased NLRP3 activation in KCs isolated from mouse livers. In addition, IL-1 $\beta$  production was reduced in Nrf2-overexpressing BMDMs, while treatment with a YAP inhibitor abrogated the effects of Nrf2 overexpression. Taken together, these results indicate that Nrf2 can regulate Hippo signaling in macrophages, which in turn inhibits NLRP3 inflammasome activation.

To further determine whether Nrf2 overexpression in macrophages can attenuate steatohepatitis in mouse NASH models, we administered AAV-SP-Nrf2 to WT mice exposed to HFD feeding. It has been confirmed that the SP146-C1 could express specifically in macrophages cell lines as previous described (Kang et al., 2014). Our results showed significantly improved liver inflammation and steatosis in the Nrf2-overexpression group compared with the control group. Together, these studies suggest that targeting Nrf2 activation may be a potential therapeutic strategy to delay steatohepatitis progression. We found Nrf2 overexpression could augment the YAP expression and subsequently decrease the NLRP3 activation, further confirming that Nrf2 can modulate YAP activity, which in turn regulates NLRP3 activation.

In summary, our findings obtain a comprehensive understanding of myeloid Nrf2's role in NASH progression. We demonstrated that Nrf2 plays a crucial role in YAP stabilization in an ROS-dependent manner, which in turn inhibits NLRP3 inflammasome activation, leading to improved symptoms of steatohepatitis. Therefore, we believe our study paves a new path to NASH's clinical treatment strategies by targeting macrophage Nrf2.

**Limitations of the study**

There are some limitations to this study. Our data demonstrated YAP activity mediation is essential for NLRP3 inflammasome activation in NASH, but the underlying mechanism remains to be explored. Second, although the YAP activator's administration is easier to carry out clinical translational research, it is not specific enough to explain the molecular mechanism *in vivo* because it influences various cell types. Third, the evidence for the role of the Nrf2-YAP-NLRP3 axis in human macrophages is lacked, which we believe could provide more direct guidance for clinical treatment in the future. Fourth, because that adipocyte is one of the leading players in NASH progression and the cross talk between adipocyte and macrophage in metabolic disorders has been gradually revealed, more experiments focusing on adipocytes might deepen the understanding of the molecular mechanism in the present study.

**Resource availability**

*Lead contact*

Further information is available from the Lead Contact, ling lv ([lvling@njmu.edu.cn](mailto:lvling@njmu.edu.cn)).

### Materials availability

Novel materials generated in this study are available from the Lead Contact on reasonable request.

### Data and code availability

The data that support the findings of this study are available from the Lead Contact on reasonable request.

## METHODS

All methods can be found in the accompanying [Transparent Methods supplemental file](#).

## SUPPLEMENTAL INFORMATION

Supplemental information can be found online at <https://doi.org/10.1016/j.isci.2021.102427>.

## ACKNOWLEDGMENTS

This study was supported by the National Natural Science Foundation of China [grant numbers 81871259, 81971495, 82070675] and the Research Unit of Liver Transplantation and Transplant Immunology, Chinese Academy of Medical Sciences [grant number 2019-I2M-5-035], the State Key Laboratory of Reproductive Medicine, Nanjing Medical University [SKLRM-K202001], and the Six talent peaks project in Jiangsu Province (2017-WSW-019).

## AUTHOR CONTRIBUTIONS

Literature search: Peng Wang, Ming Ni, Yizhu Tian;

Figures: Peng Wang, Jiannan Qiu; Study design: Peng Wang, Jianhua Rao, Ling Lu; Data collection: Peng Wang, Ming Ni, Yizhu Tian, Jiannan Qiu, Song Wei, Yong Shi; Data analysis: Peng Wang, Yizhu Tian, Wenhua You, Hao Wang, Jinren Zhou, Lei Zhang; Data interpretation: Feng Cheng, Jianhua Rao, Ling Lu; Writing original draft: Peng Wang; Writing draft: Peng Wang, Ming Ni, Yizhu Tian, Jiannan Qiu; Jianhua Rao, Ling Lu;

## DECLARATION OF INTERESTS

The authors in the research declared that they have no conflict of interest concerning this manuscript.

Received: December 21, 2020

Revised: February 14, 2021

Accepted: April 9, 2021

Published: May 21, 2021

## REFERENCES

- Azzimato, V., Jager, J., Chen, P., Morgantini, C., Levi, L., Barreby, E., Sulen, A., Oses, C., Willerbrords, J., Xu, C., et al. (2020). Liver macrophages inhibit the endogenous antioxidant response in obesity-associated insulin resistance. *Sci. Transl. Med.* *26* (532), 12.
- Basu, S., Totty, N.F., Irwin, M.S., Sudol, M., and Downward, J. (2003). Akt phosphorylates the Yes-associated protein, YAP, to induce interaction with 14-3-3 and attenuation of p73-mediated apoptosis. *Mol. Cell* *11*, 11–23.
- Beier, K., Volkl, A., and Fahimi, H.D. (1992). Suppression of peroxisomal lipid beta-oxidation enzymes of TNF-alpha. *FEBS Lett.* *310*, 273–276.
- Beier, K., Völkl, A., and Fahimi, H.D. (1997). TNF-alpha downregulates the peroxisome proliferator activated receptor-alpha and the mRNAs encoding peroxisomal proteins in rat liver. *FEBS Lett.* *412*, 385–387.
- Bellezza, I., Giambanco, I., Minelli, A., and Donato, R. (2018). Nrf2-Keap1 signaling in oxidative and reductive stress. *Biochim. Biophys. Acta Mol. Cell Res.* *1865*, 721–733.
- Cai, C., Zhu, X., Li, P., Li, J., Gong, J., Shen, W., and He, K. (2017). NLRP3 deletion inhibits the non-alcoholic steatohepatitis development and inflammation in kupffer cells induced by palmitic acid. *Inflammation* *40*, 1875–1883.
- Cucci, M.A., Grattarola, M., Dianzani, C., Damia, G., Ricci, F., Roetto, A., Trotta, F., Barrera, G., and Pizzimenti, S. (2020). Ailanthone increases oxidative stress in CDDP-resistant ovarian and bladder cancer cells by inhibiting of Nrf2 and YAP expression through a post-translational mechanism. *Free Radic. Biol. Med.* *150*, 125–135.
- Dodson, M., de la Vega, M.R., Cholanians, A.B., Schmidlin, C.J., Chapman, E., and Zhang, D.D. (2019). Modulating NRF2 in disease: timing is everything. *Annu. Rev. Pharmacol. Toxicol.* *59*, 555–575.
- Estes, C., Anstee, Q.M., Arias-Loste, M.T., Bantel, H., Bellentani, S., Caballeria, J., Colombo, M., Craxi, A., Crespo, J., and Day, C.P. (2018). Modeling NAFLD disease burden in China, France, Germany, Italy, Japan, Spain, United Kingdom, and United States for the period 2016–2030. *J. Hepatol.* *69*, 896–904.
- Font-Burgada, J., Sun, B., and Karin, M. (2016). Obesity and cancer: the Oil that feeds the flame. *Cell Metab.* *23*, 48–62.
- Friedman, S.L., Neuschwander-Tetri, B.A., Rinella, M., and Sanyal, A.J. (2018). Mechanisms of NAFLD development and therapeutic strategies. *Nat. Med.* *24*, 908–922.
- Han, Y.H., Kim, H.J., Na, H., Nam, M.W., Kim, J.Y., Kim, J.S., Koo, S.H., and Lee, M.O. (2017). ROR $\alpha$  induces KLF4-mediated M2 polarization in the

- liver macrophages that protect against nonalcoholic steatohepatitis. *Cell Rep.* 20, 124–135.
- Hayes, J.D., and Dinkova-Kostova, A.T. (2014). The Nrf2 regulatory network provides an interface between redox and intermediary metabolism. *Trends Biochem. Sci.* 39, 199–218.
- Huang, W., Metlakunta, A., Dedousis, N., Zhang, P., Sipula, I., Dube, J.J., Scott, D.K., and O’Doherty, R.M. (2010). Depletion of liver Kupffer cells prevents the development of diet-induced hepatic steatosis and insulin resistance. *Diabetes* 59, 347–357.
- Ibrahim, S.H., Hirsova, P., and Gores, G.J. (2018). Non-alcoholic steatohepatitis pathogenesis: sublethal hepatocyte injury as a driver of liver inflammation. *Gut* 67, 963–972.
- Kang, W.S., Kwon, J.S., Kim, H.B., Jeong, H.Y., Kang, H.J., Jeong, M.H., Cho, J.G., Park, J.C., Kim, Y.S., and Ahn, Y. (2014). A macrophage-specific synthetic promoter for therapeutic application of adiponectin. *Gene Ther.* 21, 353–362.
- Kazankov, K., Jørgensen, S.M.D., Thomsen, K.L., Møller, H.J., Vilstrup, H., George, J., Schuppan, D., and Grønbaek, H. (2019). The role of macrophages in nonalcoholic fatty liver disease and nonalcoholic steatohepatitis. *Nat. Rev. Gastroenterol. Hepatol.* 16, 145–159.
- Ke, B., Shen, X.D., Zhang, Y., Ji, H., Gao, F., Yue, S., Kamo, N., Zhai, Y., Yamamoto, M., Busuttill, R.W., and Kupiec-Weglinski, J.W. (2013). KEAP1-NRF2 complex in ischemia-induced hepatocellular damage of mouse liver transplants. *J. Hepatol.* 59, 1200–1207.
- Klaassen, C.D., and Reisman, S.A. (2010). Nrf2 the rescue: effects of the antioxidative/electrophilic response on the liver. *Toxicol. Appl. Pharmacol.* 244, 57–65.
- Kobayashi, E.H., Suzuki, T., Funayama, R., Nagashima, T., Hayashi, M., Sekine, H., Tanaka, N., Moriguchi, T., Motohashi, H., Nakayama, K., and Yamamoto, M. (2016). Nrf2 suppresses macrophage inflammatory response by blocking proinflammatory cytokine transcription. *Nat. Commun.* 7, 11624.
- Kolios, G., Valatas, V., and Kouroumalis, E. (2006). Role of Kupffer cells in the pathogenesis of liver disease. *World J. Gastroenterol.* 12, 7413–7420.
- Li, C., Jin, Y., Wei, S., Sun, Y., Jiang, L., Zhu, Q., Farmer, D.G., Busuttill, R.W., Kupiec-Weglinski, J.W., and Ke, B. (2019). Hippo signaling controls NLR family pyrin domain containing 3 activation and governs immunoregulation of mesenchymal stem cells in mouse liver injury. *Hepatology* 70, 1714–1731.
- Liu, Y., Lu, T., Zhang, C., Xu, J., Xue, Z., Busuttill, R.W., Xu, N., Xia, Q., Kupiec-Weglinski, J.W., and Ji, H. (2019). Activation of YAP attenuates hepatic damage and fibrosis in liver ischemia-reperfusion injury. *J. Hepatol.* 71, 719–730.
- Ma, Q. (2013). Role of nrf2 in oxidative stress and toxicity. *Annu. Rev. Pharmacol. Toxicol.* 53, 401–426.
- Musso, G., Gambino, R., Cassader, M., Paschetta, E., and Sircana, A. (2018). Specialized proresolving mediators: enhancing nonalcoholic steatohepatitis and fibrosis resolution. *Trends Pharmacol. Sci.* 39, 387–401.
- Neyrinck, A.M., Cani, P.D., Dewulf, E.M., De Backer, F., Bindels, L.B., and Delzenne, N.M. (2009). Critical role of Kupffer cells in the management of diet-induced diabetes and obesity. *Biochem. Biophys. Res. Commun.* 385, 351–356.
- Park, J.W., Jeong, G., Kim, S.J., Kim, M.K., and Park, S.M. (2007). Predictors reflecting the pathological severity of non-alcoholic fatty liver disease: comprehensive study of clinical and immunohistochemical findings in younger Asian patients. *J. Gastroenterol. Hepatol.* 22, 491–497.
- Patoureaux, S., Rousseau, D., Bonnafous, S., Lebeaupin, C., Luci, C., Canivet, C.M., Schneck, A.S., Bertola, A., Saint-Paul, M.C., Iannelli, A., et al. (2017). CD44 is a key player in nonalcoholic steatohepatitis. *J. Hepatol.* 67, 328–338.
- Qin, S., Du, R., Yin, S., Liu, X., Xu, G., and Cao, W. (2015). Nrf2 is essential for the anti-inflammatory effect of carbon monoxide in LPS-induced inflammation. *Inflamm. Res.* 64, 537–548.
- Rao, J., Qian, X., Li, G., Pan, X., Zhang, C., Zhang, F., Zhai, Y., Wang, X., and Lu, L. (2015). ATF3-mediated NRF2/HO-1 signaling regulates TLR4 innate immune responses in mouse liver ischemia/reperfusion injury. *Am. J. Transpl.* 15, 76–87.
- Rivera, C.A., Adegboye, P., van Rooijen, N., Tagalicud, A., Allman, M., and Wallace, M. (2007). Toll-like receptor-4 signaling and Kupffer cells play pivotal roles in the pathogenesis of non-alcoholic steatohepatitis. *J. Hepatol.* 47, 571–579.
- Rojo de la Vega, M., Chapman, E., and Zhang, D.D. (2018). NRF2 and the hallmarks of cancer. *Cancer Cell* 34, 21–43.
- Stienstra, R., Saudale, F., Duval, C., Keshtkar, S., Groener, J.E., van Rooijen, N., Staels, B., Kersten, S., and Müller, M. (2010). Kupffer cells promote hepatic steatosis via interleukin-1beta-dependent suppression of peroxisome proliferator-activated receptor alpha activity. *Hepatology* 51, 511–522.
- Szabo, G., and Csak, T. (2012). Inflammasomes in liver diseases. *J. Hepatol.* 57, 642–654.
- Tang, W., Jiang, Y.F., Ponnusamy, M., and Diallo, M. (2014). Role of Nrf2 in chronic liver disease. *World J. Gastroenterol.* 20, 13079–13087.
- Tosello-Trampont, A.C., Landes, S.G., Nguyen, V., Novobrantseva, T.I., and Hahn, Y.S. (2012). Kupffer cells trigger nonalcoholic steatohepatitis development in diet-induced mouse model through tumor necrosis factor- $\alpha$  production. *J. Biol. Chem.* 287, 40161–40172.
- Varelas, X. (2017). The Hippo pathway effectors TAZ and YAP in development, homeostasis and disease. *Development* 141, 1614–1626.
- Wang, P., Geng, J., Gao, J., Zhao, H., Li, J., Shi, Y., Yang, B., Xiao, C., Linghu, Y., Sun, X., et al. (2019). Macrophage achieves self-protection against oxidative stress-induced ageing through the Mst-Nrf2 axis. *Nat. Commun.* 10, 755.
- Wu, H., Xiao, Y., Zhang, S., Ji, S., Wei, L., Fan, F., Geng, J., Tian, J., Sun, X., Qin, F., et al. (2013). The Ets transcription factor GABP is a component of the hippo pathway essential for growth and antioxidant defense. *Cell Rep.* 3, 1663–1677.
- Yang, G., Lee, H.E., and Lee, J.Y. (2016). A pharmacological inhibitor of NLRP3 inflammasome prevents non-alcoholic fatty liver disease in a mouse model induced by high fat diet. *Sci. Rep.* 6, 24399.
- Younossi, Z., Anstee, Q.M., Marietti, M., Hardy, T., Henry, L., Eslam, M., George, J., and Bugianesi, E. (2018). Global burden of NAFLD and NASH: trends, predictions, risk factors and prevention. *Nat. Rev. Gastroenterol. Hepatol.* 15, 11–20.
- Zhou, Y., Huang, T., Zhang, J., Cheng, A.S.L., Yu, J., Kang, W., and To, K.F. (2018). Emerging roles of Hippo signaling in inflammation and YAP driven tumor immunity. *Cancer Lett.* 426, 73–79.
- Zhou, Y., Wang, K., Zhou, Y., Li, T., Yang, M., Wang, R., Chen, Y., Cao, M., and Hu, R. (2019). HEATR1 deficiency promotes pancreatic cancer proliferation and gemcitabine resistance by up-regulating Nrf2 signaling. *Redox Biol.* 29, 101390.

**Supplemental information**

**Myeloid Nrf2 deficiency aggravates non-alcoholic steatohepatitis progression by regulating YAP-mediated NLRP3 inflammasome signaling**

**Peng Wang, Ming Ni, Yizhu Tian, Hao Wang, Jiannan Qiu, Wenhua You, Song Wei, Yong Shi, Jinren Zhou, Feng Cheng, Jianhua Rao, and Ling Lu**

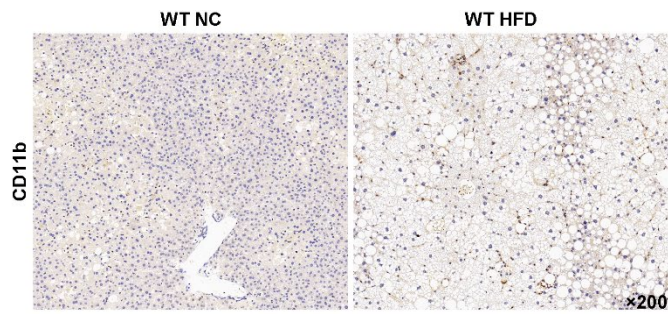


**Figure S1. The effects of HFD feeding on macrophages infiltration in wild type mice livers (Related to Figure 1).**

Immunohistochemical staining of CD11b<sup>+</sup> macrophages in mice livers obtained from HFD group or Normal group (magnification×200). N=6 mice/group.

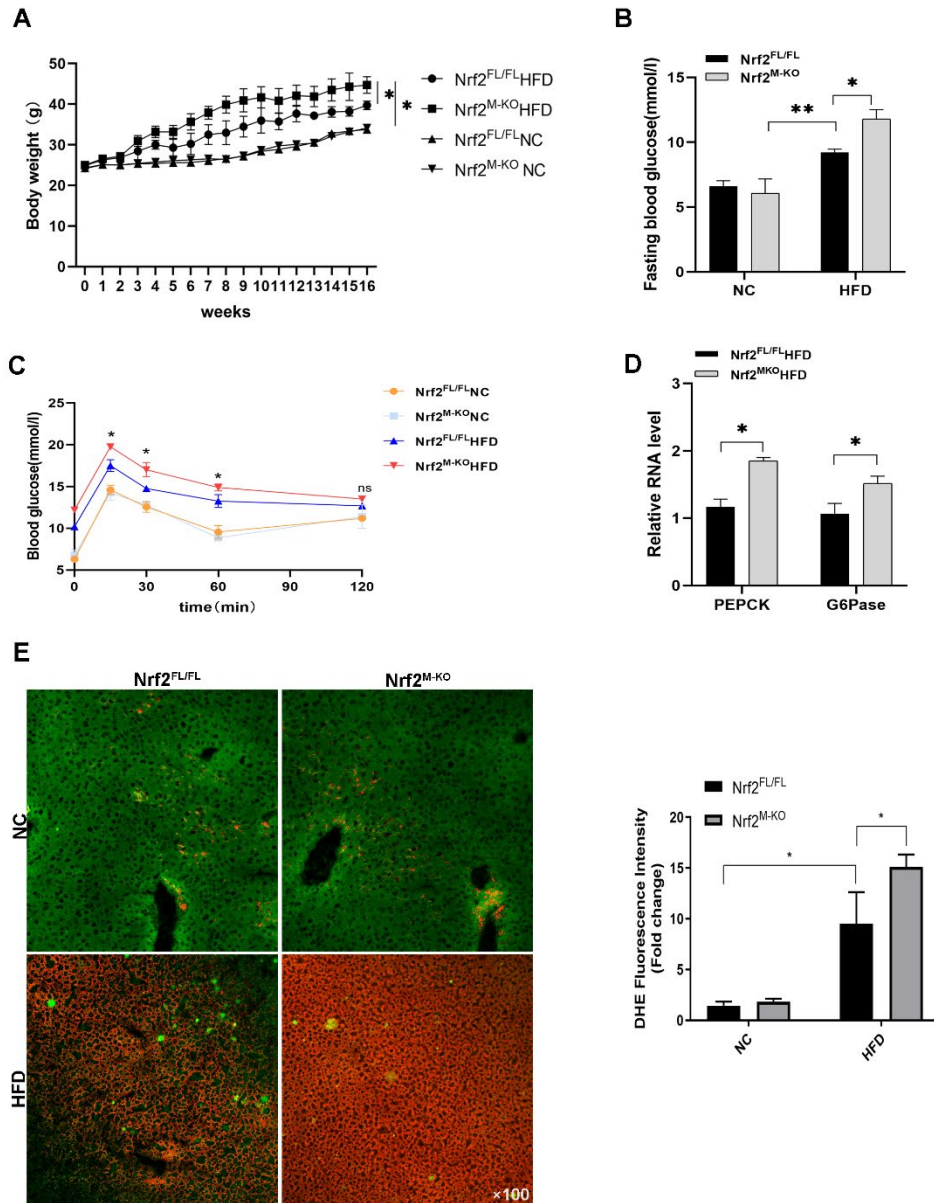


**Figure S2. Effects of macrophage Nrf2 depletion on body weight, glucose tolerance, hepatic gluconeogenesis and livers ROS contents during HFD feeding (Related to Figure 2).**

(A) Body weight. (B) and (C) Fasting blood glucose and Intraperitoneal glucose tolerance test (GTT). (D) The gene expression of PEPCK and G6Pase in NASH livers.

(E) The DHE staining of mice livers. N=6 mice/group. Data are expressed as mean  $\pm$  SD. \* $p < 0.05$  versus Nrf2<sup>FL/FL</sup> mice +HFD group (one-way ANOVA and unpaired t

student test).

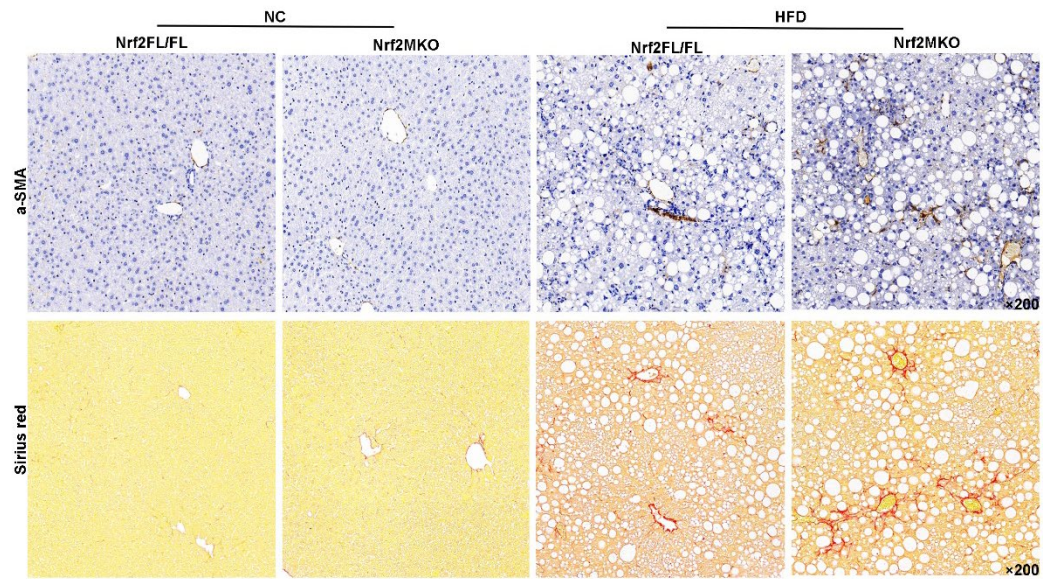


**Figure S3. Effects of macrophage Nrf2 depletion on HFD-induced liver fibrosis (Related to Figure 3).**

Immunohistochemical staining of  $\alpha$ -SMA and Sirius red staining in livers section (magnification  $\times 200$ ). N=6 mice/group.

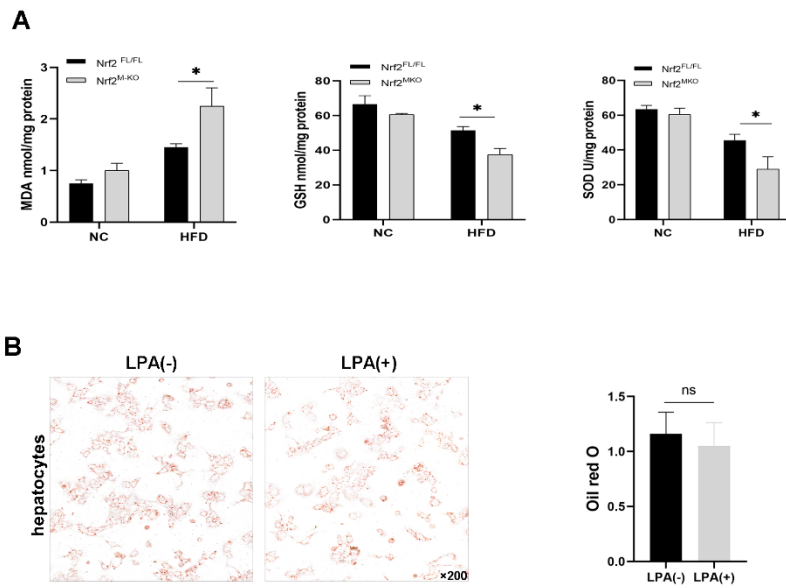


**Figure S4. Effects of macrophage Nrf2 depletion on antioxidation activity and the effects of LPA on lipid accumulation in hepatocytes (Related to Figure 2 and Figure 6).**

(A) The MDA level and GSH content and SOD activity in the liver of Nrf2<sup>FL/FL</sup> and Nrf2<sup>M-KO</sup> mice fed with HFD or NC (n=6). (B) Oil Red O Staining of palmitic acid-treated hepatocytes supplemented with LPA or not (n=4). Data are expressed as mean  $\pm$  SD. \*p<0.05 versus Nrf2<sup>FL/FL</sup> mice+ HFD group (one-way ANOVA).

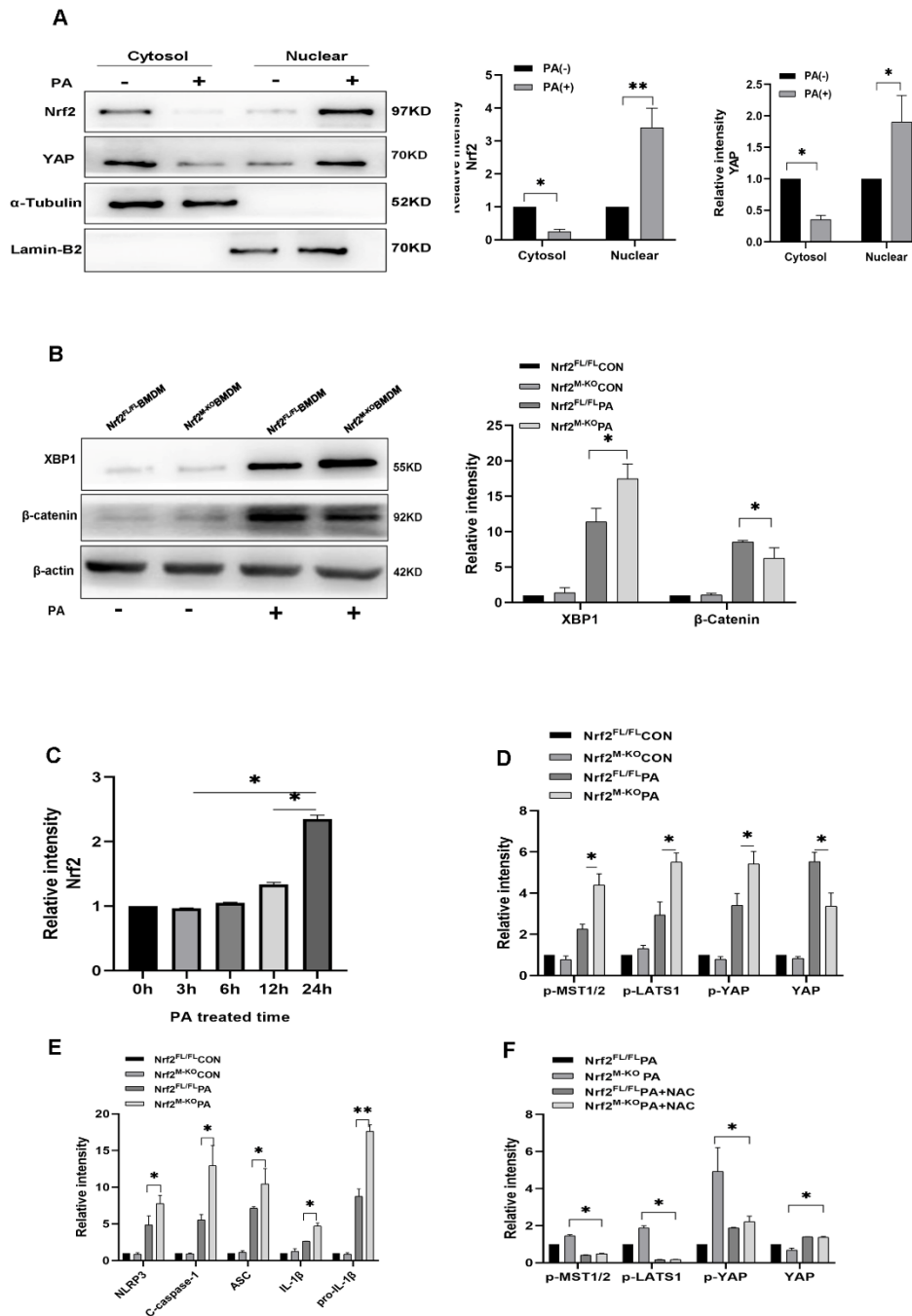


**Figure S5. Effect of PA treatment on YAP and Nrf2 translocate in the nuclear and Effect of Nrf2 deficiency on  $\beta$ -Catenin/XBP1 expressions in macrophages (Related to Figure 5).**

(A) Western blot analysis of cytosol and nuclear YAP and Nrf2 in macrophages after PA treatment. (B) Western blot analysis of XBP1 and  $\beta$ -Catenin in different groups of

BMDMs. (C) and (D) Relative ratio of macrophage Nrf2, p-MST1/2, p-LATS1, p-YAP, YAP. (E) Relative ratio of macrophage NLRP3, cleaved caspase-1, pro-caspase-1, ASC, IL-1 $\beta$ , pro-IL-1 $\beta$ . (F) Relative ratio of macrophage p-MST1/2, p-LATS1, p-YAP, YAP. N=3. Data are expressed as mean  $\pm$  SD. \*p<0.05 versus vehicle (one-way ANOVA).

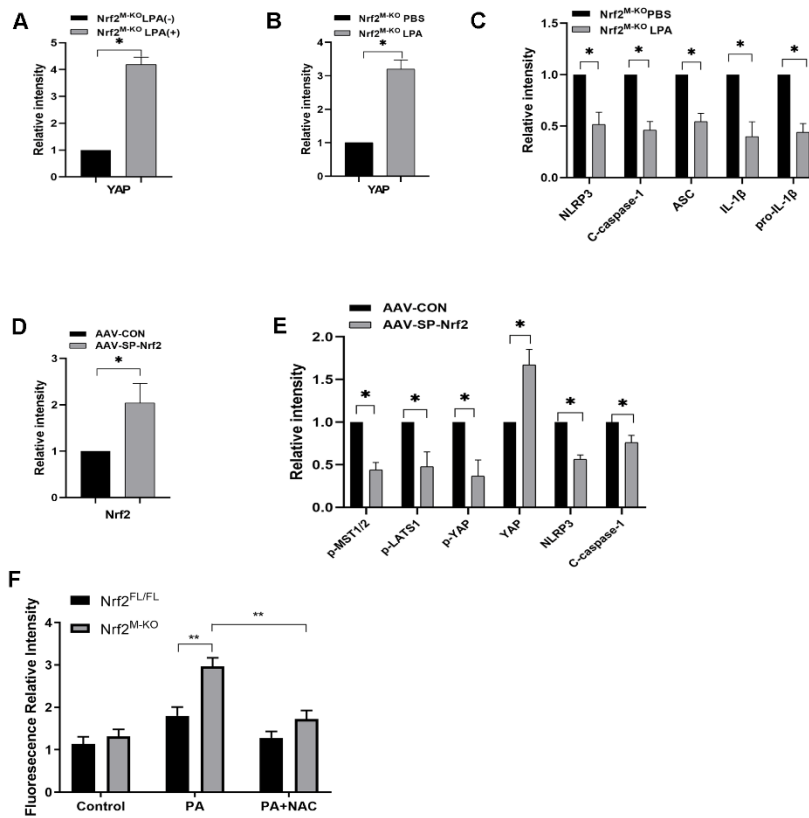


**Figure S6. The quantification analysis about the Immunoblot results and ROS contents (Related to Figure 5, Figure 7 and Figure 8).**

(A) and (B) Relative ratio of macrophage YAP. (C) Relative ratio of macrophage NLRP3, cleaved caspase-1, pro-caspase-1, ASC, IL-1 $\beta$ , pro-IL-1 $\beta$ . (D) Relative ratio of macrophage Nrf2. (E) Relative ratio of macrophage p-MST1/2, p-LATS1, p-YAP, YAP, NLRP3, C-caspase-1. (F) The quantification analysis of ROS contents in macrophages. N=3. Data are expressed as mean  $\pm$  SD. \* $p < 0.05$  versus vehicle (unpaired t student test).

**Figure S7**

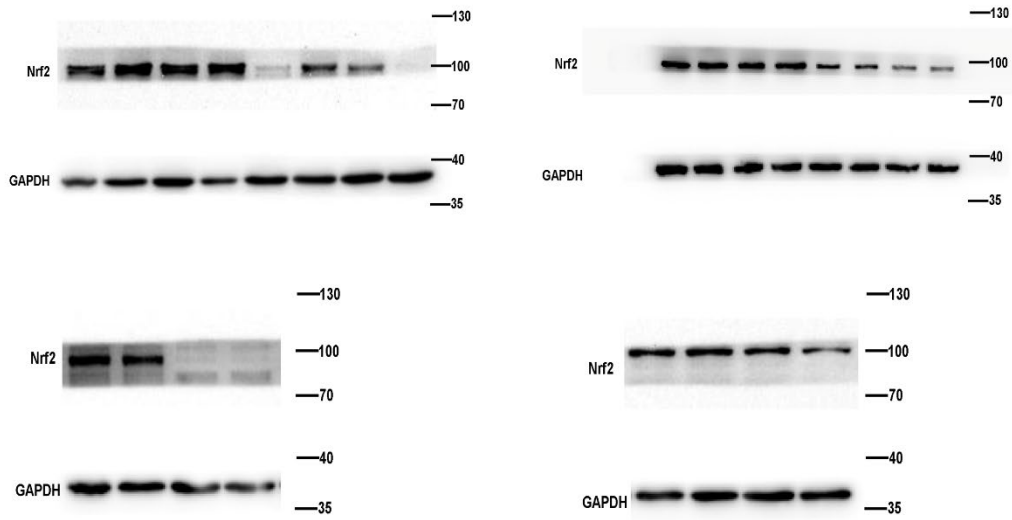


**Figure S7. Uncropped images of blots presented in main Figure 1.**

**Figure S8**

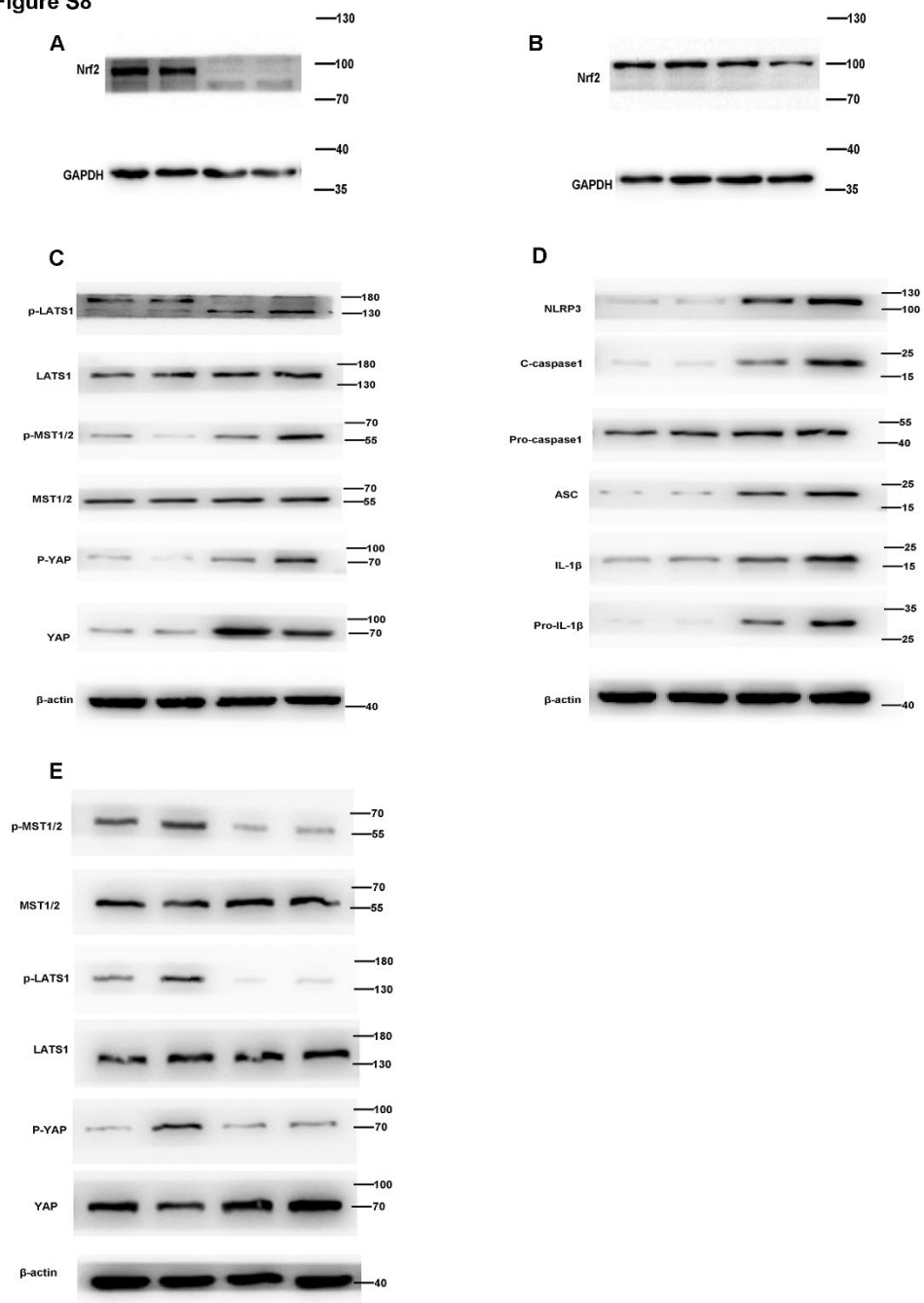


**Figure S8. Uncropped images of blots presented in main Figure 5.**

**Figure S9**

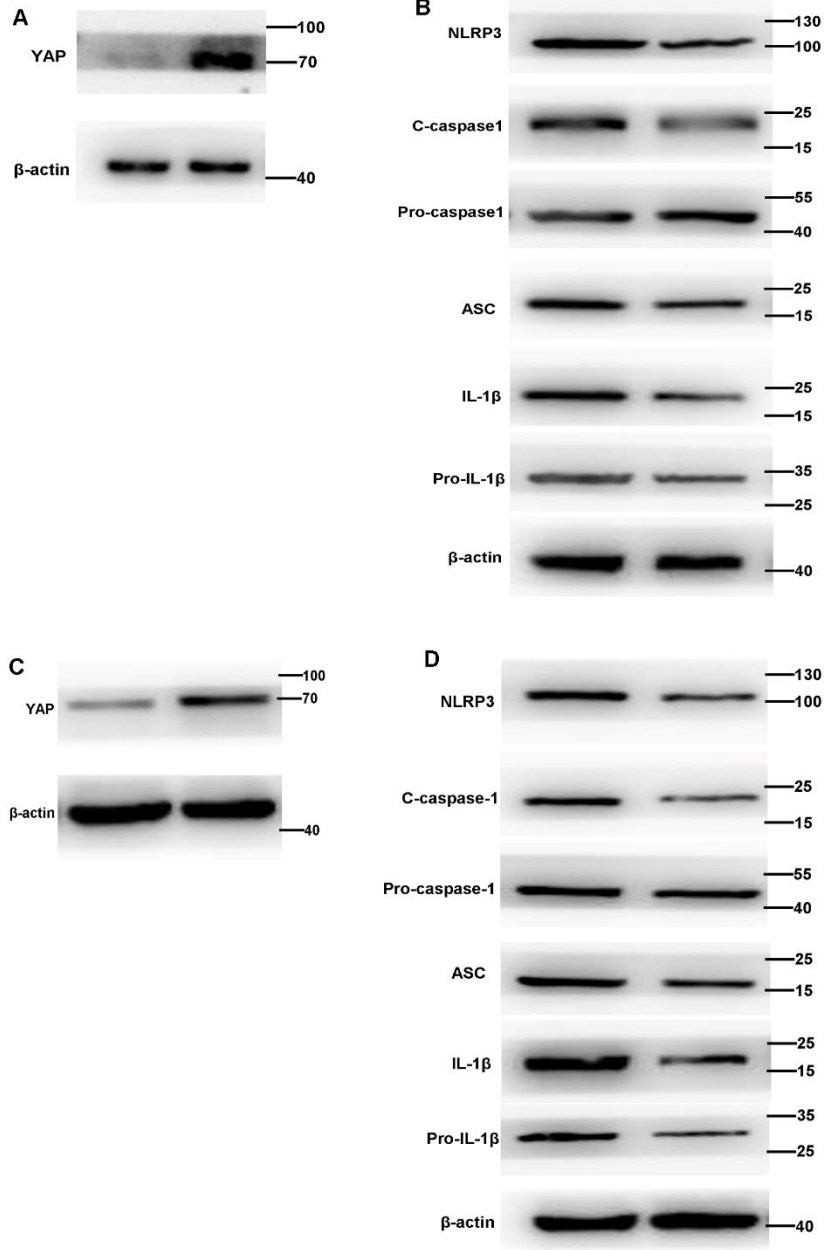


**Figure S9. Uncropped images of blots presented in main Figure 6 and 7**

Figure S10

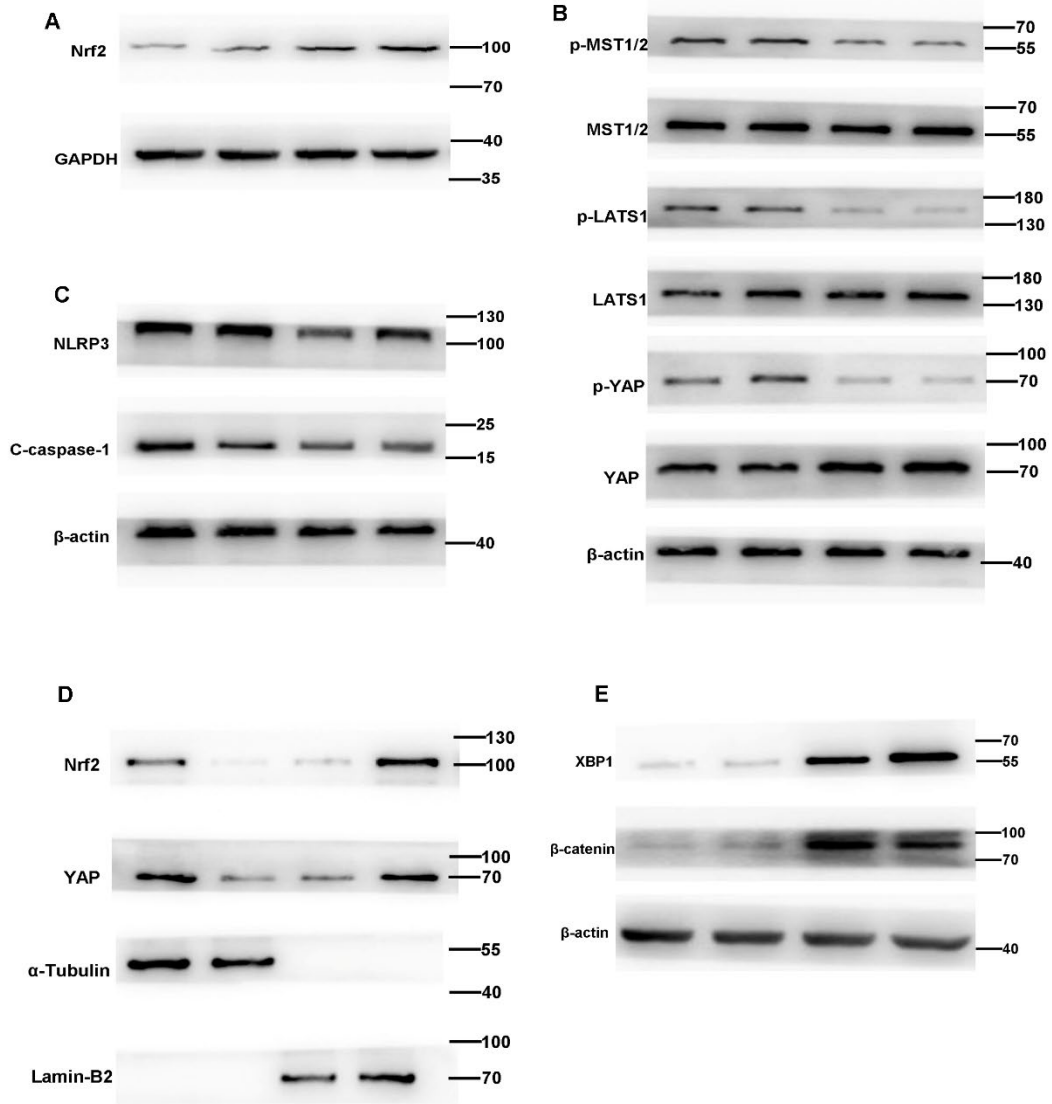


**Figure S10. Uncropped images of blots presented in main Figure 8 and supplementary Figure 5.**

**TableS1. Primer sequences (Related to Figure 1-8).**

Gene Symbol	Forward Primer	Reverse Primer
Mus-Nrf2	TAGATGACCATGAGTCGCTTGC	GCCAAACTTGCTCCATGTCC
Mus-TNF-a	CTGAACTTCGGGGTGATCGG	GGCTTGTCACCTCGAATTTTGAGA
Mus-IL-6	CTGCAAGAGACTTCCATCCAG	AGTGGTATAGACAGGTCTGTTGG
Mus-IL-1 $\beta$	GCAACTGTTTCTGAACTCAACT	ATCTTTTGGGGTCCGTCAACT
Mus-IL-4	GGTCTCAACCCCGAGTAGT	GCCGATGATCTCTCTCAAGTGAT
Mus-IL-10	CTTACTGACTGGCATGAGGATCA	GCAGCTCTAGGAGCATGTGG
Mus-CXCL10	CCAAGTGCTGCCGTCATTTTC	GGCTCGCAGGGATGATTTCAA
Mus-FAS	CTGCGATTCTCTGGCTGTGAA	CAACAACCATAGGCGATTCTGG
Mus-SREBP1c	GCAGCCACCATCTAGCCTG	CAGCAGTGAGTCTGCCTTGAT
Mus- Pparg	GGAAGACCACTCGCATTCCCTT	GTAATCAGCAACCATTGGGTCA
Mus-Fabp4	AAGGTGAAGAGCATCATAACCCT	TCACGCCTTTCATAACACATTCC
Mus-Cpt1a	CTCCGCCTGAGCCATGAAG	CACCAGTGATGATGCCATTCT
Mus-Cyp4a14	TTTAGCCCTACAAGGTAAGTGGGA	GCAGCCACTGCCTTCGTAA
Mus- Acadl	AACACAACACTCGAAAGCGG	TTCTGCTGTTCCGTCAACTCA
Mus- Ppara	AACATCGAGTGTCGAATATGTGG	CCGAATAGTTCGCCGAAAGAA
Mus-GAPDH	AGGTCGGTGTGAACGGATTTG	TGTAGACCATGTAGTTGAGGTCA
Mus- $\beta$ -actin	GTGACGTTGACATCCGTAAAGA	GCCGGACTCATCGTACTCC
Hum-Nrf2	TCAGCGACGGAAAGAGTATGA	CCACTGGTTTCTGACTGGATGT
Hum-GAPDH	GGAGCGAGATCCCTCCAAAAT	GGCTGTTGTCATACTTCTCATGG

**TableS2. Information about the patients (Related to Figure 1).**

VARIABLES	PATIENTS WITH NASH	Control
N	4	4
SEX(MALE/FEMAL)	1/3	2/2
DISEASE	HEPATIC HEMANGIOMA (2) HEPATIC CYST (2)	HEPATIC HEMANGIOMA (2) HEPATIC CYST (2)
BMI (kg/m <sup>2</sup> )	28.0(25-30)	23.9(22-25)
Obesity	4	1
Type2 diabetes	3	0
Consumption of alcohol (>15g/day)	0	0
TG (mmol/L)	3.3(2.1-3.9)	1.5(1.2-1.8)
ALT (U/L)	87(67-100)	30(25-45)
AST(U/L)	100(80-123)	27(25-37)
Fasting blood glucose (mmol/L)	8.3(6.7-9.5)	4.5(4.0-5.3)

**TableS3. NAS score in Figure 2D(Related to Figure 2).**

Nrf2 <sup>FL/FL</sup> HFD	Nrf2 <sup>M-KO</sup> HFD
6	8
6	8
5	7
5	6
6	8
5	8

**Key Resources Table (Related to Figure 1-8).****a. Primary antibodies.**

Reagents	Source	Incubation
Nrf2	Abcam, RRID: AB_2715528	1:1000, 4°C, overnight
YAP	CST, RRID: AB_2650491	1:1000, 4°C, overnight
p-MST1/2	CST, RRID: AB_330269	1:1000, 4°C, overnight
MST1/2	CST, RRID: AB_2144632	1:1000, 4°C, overnight
p-LATS1	CST, RRID: AB_2133515	1:1000, 4°C, overnight
LATS1	CST, RRID: AB_2296754	1:1000, 4°C, overnight
p-YAP	CST, RRID: AB_2218913	1:1000, 4°C, overnight
NLRP3	CST, No RRID.	1:1000, 4°C, overnight
ASC	CST, No RRID	1:1000, 4°C, overnight
Pro-Caspase-1	CST, RRID: AB_2243894	1:1000, 4°C, overnight
Caspase-1	CST, RRID: AB_2243894	1:1000, 4°C, overnight
Pro-IL-1 $\beta$	CST, No RRID	1:1000, 4°C, overnight
IL-1 $\beta$	CST, RRID: AB_2737350	1:1000, 4°C, overnight
GAPDH	CST, RRID: AB_10622025	1:1000, 4°C, overnight
$\beta$ -actin	CST, RRID: AB_330288	1:1000, 4°C, overnight
XBP1	CST, RRID: AB_2687943	1:1000, 4°C, overnight
$\alpha$ -Tubulin	CST, No RRID.	1:1000, 4°C, overnight

**b. Secondary Antibodies.**

Reagents	Source	Incubation
Alexa Fluor 594-conjugated anti-rabbit IgG	Abcam	1:200, RT, 2hours
goat anti-rabbit	Thermo Fisher Scientific	1:2000, RT, 2hours
goat anti-rat	Thermo Fisher Scientific	1:2000, RT, 2hours

**c. Dye.**

Reagents	Source	Incubation
Oil-red O solution	Sigma Aldrich	20 minutes
H2DCFDA	Invitrogen	20 minutes
Dihydroethidium	Fushen, Shanghai	1:1000, 30minutes

**d. Diets.**

Diets	Source	Catalog
Normal chow	Research diets	D09100304
High fat Diet	Research diets	D09100310

**e. Chemicals**

Reagents	Source
Palmitic acid	Sigma Aldrich
Bovine serum albumin	Sigma Aldrich
1-oleoyl lysophosphatidic acid	Toctris Bioscience
verteporfin	MedChemExpress
type IV collagenase	Sigma Aldrich

Percoll	Sigma Aldrich
---------	---------------

## **Transparent Methods**

### **Animals study and Human liver samples**

The Nrf2<sup>FL/FL</sup> mice and Lyz2Cre-Nrf2<sup>FL/FL</sup> mice were purchased from the Model Animal Research Center of Nanjing University. Both male 8-10 weeks old Nrf2<sup>FL/FL</sup> and Nrf2<sup>M-KO</sup> mice were fed with either normal chow or HFD diets (Research diets, US) for 16 weeks. All mice were housed under specific pathogen-free condition at 23 ± 1 °C with a 12-h light-dark cycle. The YAP activator (1-oleoyl lysophosphatidic acid [LPA, 0.8umol/ kg, i.v, Tocris Bioscience, Minneapolis]) were administrated in Nrf2<sup>M-KO</sup> mice after 8 weeks HFD feeding. Mice were sacrificed at the end of 16 weeks HFD feeding and the liver and serum samples were collected for analysis. All animal experiments have been approved by the Institutional Animal Care and Use Committee of Nanjing Medical University. The human liver samples were collected from patients with NAFLD who undergo hepatectomy due to benign liver diseases such as hepatic cysts or hepatic hemangioma. All the patients were informed and consented the collection of liver samples.

### **Cell isolation and Cell Culture**

Primary hepatocytes were obtained from 8-10 weeks male mice. First, the liver was perfused with warm PBS and Hank's balanced salt solution containing 1 mg/ml type IV collagenase (Sigma-Aldrich), then liver suspension was centrifugated and the sediment was preserved, resuspended the sediment in 40% Percoll and centrifugated in 500 x g for 15 minutes, the cells in the bottom was collected for further research (Srivastava et

l., 2012). For liver macrophages, the liver suspension was obtained by adhering the step in the upper methods, then the supernatant was collected and centrifuged 650 x g for 7 minutes, abandoned the supernatant and resuspended in 10ml DME medium, added the cells in 50%/25% Percoll and centrifuged 1800 x g for 15 minutes to obtain the macrophages (Yu and Liu, 2019). BMDMs were isolated from the bone marrow from Nrf2<sup>FL/FL</sup> and Nrf2<sup>M-KO</sup> mice and then cultured in DMEM contained 10% fetal bovine serum supplemented with 20 ng/mL macrophage colony stimulating factor (M-CSF) (Sino Biologic, Beijing, China) for 7 days to fully differentiate macrophages. The human liver samples were digested by Pronase under continuous control of pH. Then Nycodenz gradient centrifugation were used to separate the human Kupffer cells from other non-parenchymal cells (Malaguarnera et al., 2006). Cells were stimulated with palmitic acid (PA, 200 $\mu$ M, Sigma-Aldrich) coupled with bovine serum albumin (BSA, Sigma-Aldrich). The cells were treated with 1-oleoyl lysophosphatidic acid (LPA, 10 $\mu$ M, Tocris Bioscience, Minneapolis) or verteporfin (VP, 10 $\mu$ M, MedChemExpress, USA).

### **Western blot analysis**

The liver tissues or cells were collected to extract proteins by using lysis buffer (RIPA, Beyotime biotechnology) according to the manufacturer's instructions. Western blot were performed with antibodies against Nrf2 (1:1000, Abcam, USA), YAP, p-YAP, p-MST1/2, MST1/2, p-LATS1, LATS1, NLRP3, cleaved caspase-1, ASC, pro-caspase-1, ASC, IL-1 $\beta$ , pro-IL-1 $\beta$  (1:1000; Cell Signaling Technology, USA), GAPDH and  $\beta$ -actin,  $\alpha$ -Tubulin (1:1000; Cell Signaling Technology, USA). ImageJ software was used

to quantify the protein expression and  $\beta$ -Actin or GAPDH was used as the control.

### **Real-time quantitative PCR**

In brief, total RNA was extracted from liver tissues or cells for cDNA synthesis using the TRIzol reagent (Invitrogen). After cDNA synthesis, the expressions of indicated genes were detected by real-time PCR using the SYBR Green master mix (Vazyme, Nanjing, China). The PCR results of GAPDH served as internal controls. The primers used for PCR are listed in Supplementary Table 1.

### **Analysis of liver enzymes and Enzyme-linked immune absorbance assay (ELISA)**

The serum alanine aminotransferase (ALT) and aspartate aminotransferase (AST) were detected by using the automated chemical analyzer (Olympus, Tokyo, Japan). The mice serum or cell culture supernatants were collected and measured the cytokines (TNF- $\alpha$ , IL-6, IL-1 $\beta$ , CXCL10, IL-4, IL-10) level through using ELISA kits (e Bioscience, San Diego, USA) according to the manufacturer's protocols.

### **Fasting blood glucose and Intraperitoneal glucose tolerance test (GTT)**

The fasting blood glucose was examined after all mice had fasted for 6h by glucometer. The glucose (1 g/kg, Sigma-Aldrich, USA) was i.p. injected into mice and then the blood glucose was examined at 0, 30, 60 and 120 min after injection.

### **ROS accumulation detection with H2DCFDA staining and DHE staining**

Intracellular ROS levels in BMDMs were measured using 2',7'-dichlorofluorescein diacetate (H2DCFDA; Invitrogen) according to the manufacturer's instructions. The BMDMs were added with 2 mM H2DCFDA for 20 min at 37 °C in dark after 24h PA treatment. Then the DCF fluorescence intensity was detected by fluorescence

microscope (Nikon, Japan). The fresh liver sections were stained with Dihydroethidium (1:1000, Fushen, Shanghai) for 30mins. Then the fluorescence intensity was detected by Fluorescence confocal microscope.

### **Histological Analysis and Cell immunofluorescence staining**

Paraffin-embedded liver sections were stained with H&E to evaluate the histological changes, NALFLD activity score (NAS) Estimation were carried out based on the sum of steatosis, inflammation and hepatocyte ballooning under the microscope as previously described (Dennis and Moucht, 2020).

For Oil Red O staining, the frozen liver section(10 $\mu$ m) and the primary hepatocytes were washed with 60% isopropanol and then were stained with Oil-red O solution (Sigma Aldrich) for 20 mins. Lastly, we use 60% isopropanol to wash redundant Oil-red O solution. The nuclei were stained with hematoxylin in frozen liver section. For semi-quantitative analysis of Oil Red O staining, 1 ml 60% isopropanol were used to dissolve the Oil red O staining in cells and absorbance was detected through a spectrophotometer at 518 nm.

For immunohistochemistry, paraffin-embedded liver sections were stained with antibody CD11b and Ly6G,  $\alpha$ -SMA (1:200, Cell Signaling Technology, USA) (Zhang et al., 2019).

For Sirius red staining, paraffin-embedded liver sections were stained with picrosirius Red (Abcam, USA) for 1 h.

Immunofluorescence staining of BMDMs was performed using appropriate antibody (YAP), after incubation with the indicated primary antibodies overnight at 4°C, then

Alexa Fluor 594-conjugated anti-rabbit IgG (1:200, Abcam) were added to the sections to visualize the staining. DAPI was used for nuclear counterstaining.

### **Measurement of Triglycerides and TBARS, MDA, GSH, SOD Contents in liver tissues**

Liver Tissue (100 mg) were homogenized in 1 mL solution of 5% Nonidet P 40 Substitute and water. And heat the samples to 80–100 °C in a water bath for 2–5 minutes, then cool to room temperature. Repeat the heating one more time to solubilize all triglyceride. Centrifuge for 2 minutes at top speed to remove insoluble material. The levels of total TG in the liver supernatants were assessed using Triglyceride Quantification Kit (Sigma-Aldrich, US) adhering by the manufacturer's instructions. The TBARS, MDA, GSH, SOD contents were measured by using commercial assay kit (Jian Chen, Nanjing) according to manufactures' instruction.

### **Adeno-associated virus (AAV) and lentivirus**

The AAV-SP146-C1-Nrf2 (AAV-SP-Nrf2), AAV-CONTROL (AAV-CON), lenti-Nrf2 and lenti-con were purchased from Gene Pharma (Shanghai, China). And AAV solution (108 IFU) were injected through tail vein at beginning and in the middle of 16 weeks high-fat-diet feeding as previous described [49]. Lentivirus transfection of cells was carried out by using Lipofectamine 3000 (Thermo Fisher Scientific, MA, USA) adhering the manufacture's protocol. We confirmed the efficiency of transfection by using qPCR.

### **Statistical analysis**

The values are presented as mean  $\pm$  SD. One-way ANOVA followed by Tukey-Kramer

multiple comparisons test and two-tailed Student's t test was performed in Prism 8 software for the statistical analysis. P value < 0.05 was considered as statistically significant.

### **Supplementary Reference**

Srivastava J, Siddiq A, Emdad L, Santhekadur PK, Chen D, Gredler R, et al. (2012). Astrocyte elevated gene-1 promotes hepatocarcinogenesis: novel insights from a mouse model. *Hepatology*. 56, 1782-1791.

Yu Y, Liu Y, AnW, Song J, Zhang Y, Zhao X. (2019). STING-mediated inflammation in Kupffer cells contributes to progression of nonalcoholic steatohepatitis. *The Journal of clinical investigation*. 129, 546-555.

Malaguarnera L, Di Rosa M, Zambito AM, dell'Ombra N, Nicoletti F, Malaguarnera M. (2006). Chitotriosidase gene expression in Kupffer cells from patients with non-alcoholic fatty liver disease. *Gut*. 55, 1313-20

Dennis A, Mouchti S, Kelly M, Fallowfield JA, Hirschfield G, Pavlides M, Banerjee R. (2020). A composite biomarker using multiparametric magnetic resonance imaging and blood analytes accurately identifies patients with non-alcoholic steatohepatitis and significant fibrosis. *Sci Rep*. 10, 15308.

Zhang Z, Xu X, Tian W, Jiang R, Lu Y, Sun Q, Fu R, He Q, Wang J, Liu Y, Yu H, Sun B. (2019). ARRB1 inhibits non-alcoholic steatohepatitis progression by promoting GDF15 maturation. *J Hepatol*. 72, 976-989.